Pure and Applied Geophysics

Pleistocene-Holocene Monogenetic Volcanism at the Malko-Petropavlovsk Zone of Transverse Dislocations on Kamchatka: Geochemical Features and Genesis

Olga Bergal-Kuvikas,[1,2,3,4] (iD) Ilya Bindeman,[3,5] Andrey Chugaev,[2] Yulia Larionova,[2] Alexander Perepelov,[6]
and Olga Khubaeva[1,4]

Abstract— The Malko-Petropavlovsk zone of transverse dislocations (MPZ) was formed on the extension of the deep Avachinsky transform fault in perpendicular relation to the subduction trench. It is a natural boundary between variously aged slabs in Kamchatka (103–105 Ma under Southern Kamchatka and 87–92 Ma under the Eastern volcanic belt). Monogenetic cinder cones in the MPZ are randomly distributed along these long-lived rupture zones. Here we present new geochemical and isotopic results of monogenetic volcanism in the MPZ. Based on whole rock and trace element geochemistry, Pb-Sr-Nd isotopic ratios of monogenetic cinder cone magmas were shown to tap the enriched mantle source (low $^{143}Nd/^{144}Nd$ isotopic ratios (0.512959–0.512999), and changed as $^{87}Sr/^{86}Sr$ (0.703356–0.703451) and $^{206}Pb/^{204}Pb$ (18.30–18.45), $^{208}Pb/^{207}Pb$ (38.00–38.12) isotopic ratios). High Nb/Yb and La/Yb ratios, without significant inputs of the slab's components (the lowest Ba, Th content), indicate decompression melting predominately. Calculations of the pressure (9–11 kbar) and temperature (1160–1240 °C) conditions using a glass thermobarometer suggest that magma of monogenetic cinder cones resided near the Moho boundary prior to eruption. This correlates with the crustal discontinuity under the MPZ according to geophysical observations (converted-wave seismic exploration and magnetotelluric sounding). The majority of well-preserved monogenetic cinder cones were formed in Holocene, after the last glaciation, but eruptions were not observed historically. This, however, suggests that similar eruptions in the MPZ may occur in the future. Given that the MPZ hosts major population centres of Kamchatka (Petropavlovsk, Elizovo, Vilyuchinks, and Paratunka: $\sim$ 250,000 people or $\sim$ 80% of the whole Kamchatkan population live in the major cities on the coastline of the MPZ), we highlight the urgent need to install a continuous monitoring system around the MPZ cones, geophysical investigation, and more serious attention from the local government and scientists. In particular, a detailed study of the MPZ regarding age, volume, and volcanic hazard assessment (pyroclastic vs extrusive) will help reduce potential risks of eruptions from monogenetic volcanoes for humans and infrastructures.

Keywords: Monogenetic, cinder, transform fault, magmatic plumbing, geochemistry, Pb–Sr–Nd isotopes, Kamchatka.

[1] Institute of Volcanology and Seismology FEB RAS, Petropavlovsk-Kamchatsky, Russia 683006. E-mail: kuvikas@mail.ru
[2] Institute of Geology of Ore Deposits, Petrography, Mineralogy and Geochemistry RAS, Moscow, Russia 119017.
[3] Fersman Mineralogical Museum RAS, Moscow, Russia 115162.
[4] Schmidt Institute of Physics of the Earth, Russian Academy of Sciences RAS, Moscow, Russia 123242.
[5] Department of Earth Sciences, 1272 University of Oregon, Eugene, OR 97403, USA.
[6] Vinogradov Institute of Geochemistry SB RAS, Irkutsk 664033, Russia.

Ⓑ Birkhäuser

1. Introduction

Volcanism in island arc settings is a dominant mechanism for formation of the crust along continental margins (Hamilton, 1994). After the initiation of plate tectonics, island arcs formed, migrated, and accreted to the continents (Ben-Avraham et al., 1981), creating complicated and often hidden tectonic structures of the geological settings along the continental margins worldwide. This is especially evident along the North-Western Pacific, particularly along the Kamchatka Peninsula, Russia (Fig. 1a) (Khanchuk et al., 2016; Konstantinovskaya, 2011). Modern volcanic fronts are superimposed on Cretaceous and younger crustal structures in the overriding Kamchatkan plate, playing a major role in magmatic distribution, along with the depth to the subducting Pacific slab. This paper is devoted to suprasubduction and largely forearc monogenetic volcanism as one of the indicators of these processes. In particular, its origin and distribution may reflect deep inner process on the slab, mantle wedge and stress regimes in the overriding plate (Emelyanova & Lelikov, 2013; Gazel et al., 2009; Nakamura, 1977). Monogenetic
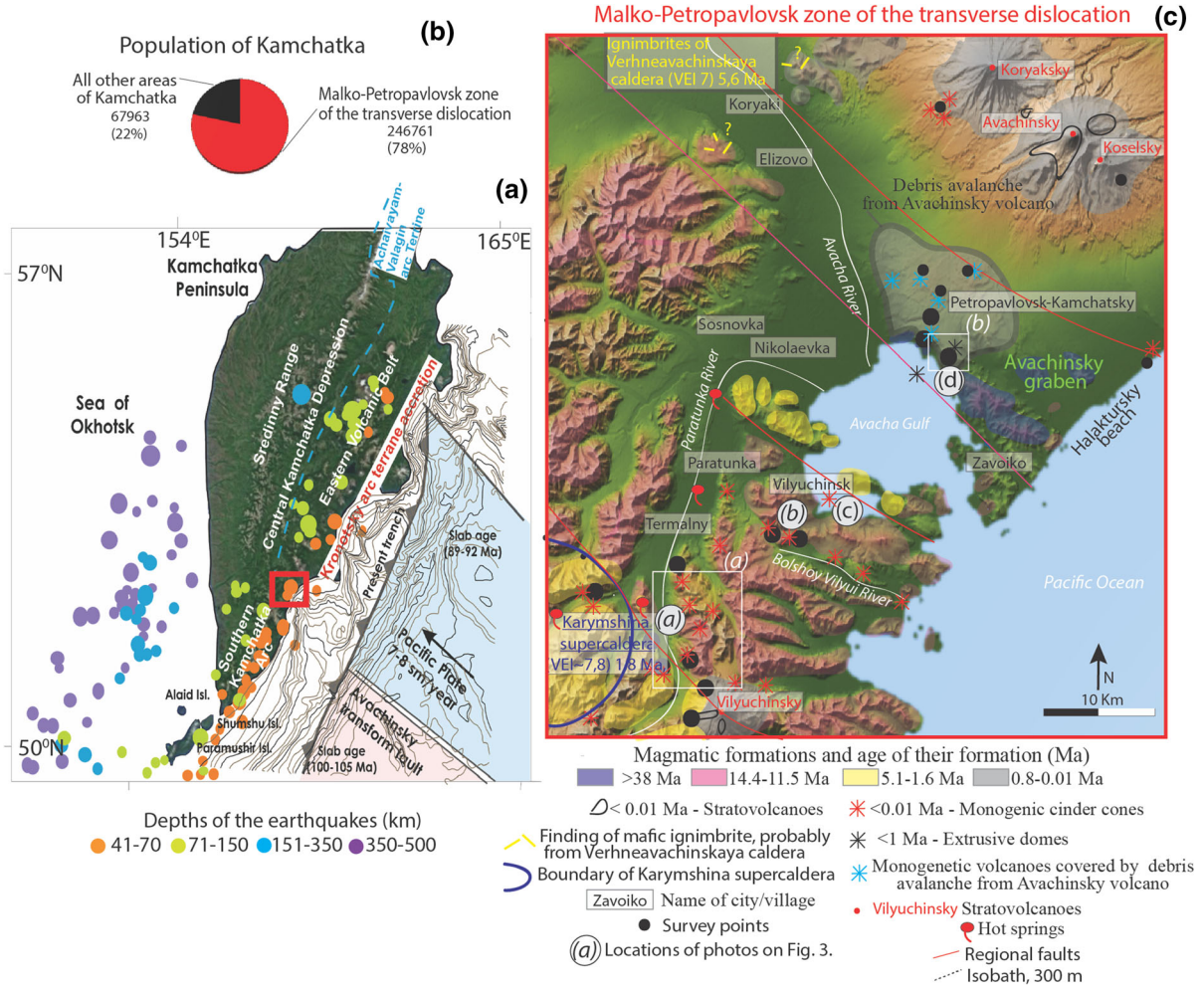
Figure 1
The present-day geodynamic setting of the Kamchatka Peninsula and the MPZ. **a** Schematic map of Kamchatka with the main volcanic belts. The position of Kronotsky arc terrane accretion is shown according to Lander & Shapiro (2007). The position of the Achaivayam-Valagin arc terrane is demonstrated according to Cherkovich and Sukhov (2005). Brown curves are isobaths on the continental slope of Kamchatka (Seliverstov, 2009). The location of the Avachinsky transform fault is illustrated by Andreev (1993). The seismological data information system collected by KBGS RAS (2020), Chebrov et al. (2013) and Chebrova et al. (2020). Ages of slabs presented by Gorbatov et al. (1997). **b** Percentage of the local population living in the MPZ and all other parts of Kamchatka based on statistical calculations of the Federal State Statistics Service (2020). Data were calculated based on the 2019 report. **c** Geological formations of the MPZ are based on the Geological map of the Russian Federation (2000), Krohin (1954) and Dirksen (2009). The boundary of the Karymshina caldera and distribution of ignimbrites of the Verkhnaevachinskaya caldera are illustrated using Bergal-Kuvikas et al. (2019) and Leonov and Rogozin (2007). Locations of cinder cone of Khlebalkina Island and extrusive dome in the Avacha Gulf are shown using Dmitriev and Ezhov (1977). The positions of the regional faults are according to the Geological map of the Russian Federation (2000). Hot spring locations are from Chudaev et al. (2016). White rectangles show the area of detailed satellite images in Fig. 2

volcanism produces small-volume volcanoes (volume of edifice ≤ 1 km^3), with a wide range of eruptive styles, such as cinder (scoria) cones, extrusive domes, maars and tuff rings (Nemeth & Kereszturi, 2015). Monogenetic volcanoes are also defined by short

eruptive periods and dispersed plumbing systems, although the magmatic systems to which they belong may be long-lived (Smith & Nemeth, 2017). Monogenetic volcanism is distributed widely and commonly represents the evolution of stress regimes

around the individual stratovolcanoes (Nemeth, 2010), but arc-perpendicular and arc-parallel linear trends of distributions of other cinder cones could be reflection of the presence of regional faults (Barde-Cabusson et al., 2014; Koyama & Umino, 1991; Maccaferri et al., 2015; Pardo et al., 2009). Future volcanic eruptions within a monogenetic volcanic field are not easy to forecast because they commonly appear at unexpected locations and sometimes use unknown faults or are not apparently associated with any known surface expression of structural elements. Furthermore, magma can migrate radially or concentrically inside the earth's crust due to stress regimes caused by inflating or deflating magmatic batches (Marti et al., 2016). Compilations of geophysical and geochemical data demonstrate that seismic activity might start 1 or 2 years before the eruption of a monogenetic volcano, but it intensifies to warning levels only 2 or 3 months or even 1 or 2 weeks prior to the eruption (Albert et al., 2016). Multiple magma batches can interact between themselves in a subvolcanic reservoir and magma plumbing system, and numerous intrusions can occur on similar time scales, as recorded by increased seismicity and gas emanation according to the seismic, petrological and geochemical monitoring (Albert et al., 2016). The above observations suggest that the study of monogenetic volcanism is difficult, but if these are associated with larger stratovolcanoes that are evolving over stable and long-lived magma sources and conduits, volcanic hazards can be combined. Monogenetic magmatism can be essential for understanding the neighbourhood of these large stratovolcanoes and providing an independent insight into the deep structure of island arcs, regional faults, and the heterogeneities of the crust. From the volcanic hazards perspective, it is important to investigate the structural control of their distribution, which often appears as random, as well as to study mechanisms of magma formation and evolution, especially in areas of high population density, as ascending magma in monogenetic eruptions may rupture at any area within a city with little warning.

Our research focus here is on the monogenetic volcanism of the Malko-Petropavlovsk zone (MPZ) in the Kamchatka Peninsula, eastern Russia and specifically on the coastline of the Avacha Gulf (Fig. 1), where the capital city of Petropavlovsk-Kamchatsky and several other cities and regional airport and infrastructures are located. The MPZ is the natural boundary between arc-parallel volcanic belts with various accretion and deformation histories and an arc-perpendicular active fault system that generates a graben-like structure (Fig. 1). The MPZ hosts massive stratovolcanoes: Avachinsky, Vilyuchinsky and Koryaksky (Fig. 1) located in arc-perpendicular arrangement. This work is the first detailed research about monogenetic volcanism in the MPZ. Here we present a new and diverse geochemical dataset for monogenetic volcanoes in an attempt to determine their origin. Furthermore, we interpret these data because they have direct implications for potential characteristics of magmatic eruptions. The primary goal of this study is to describe the distribution and investigate the origin of monogenetic volcanism in the Petropavlovsk-Kamchatsky area from the perspective of potential volcanic hazards. This research will be needed for the local population and strategic planning for cities.

2. Geodynamic and Geological Settings

2.1. Geodynamic Evolution of Kamchatka and Origin of the MPZ

The geodynamic setting of Kamchatka (Fig. 1) is in the north-western Pacific "Ring of Fire" (Trans-Pacific subduction belt). The history of Kamchatka includes accretions of the Late Cretaceous Achai-vayam-Valagin arc terrane to the Eurasian margin at the Early Eocene, $\sim$ 50 Ma (Bindeman et al., 2002; Chekhovich & Sukhov, 2006; Hourigan et al., 2009), and then the accretion of Campanian-Eocene Kronotsky arc terrane (Tsukanov et al., 2014) at 6–10 Ma (Lander & Shapiro, 2007; Levashova et al., 2000).

Deep earthquakes dominant in Southern Kamchatka and Kuriles, and their absence north of the MPZ, make a natural arc-perpendicular boundary of the Kamchatka arc (Moroz & Gontovaya, 2018) at latitude of $\sim$ 53° N (Gordeev & Bergal-Kuvikas, 2022) (Fig. 1). The possible origin of that boundary is the Avachinsky transform fault, which was estimated based on magnetic anomalies (Andreev, 1993) and

was formed due to the long evolution of the north-west Pacific convergent margin (Seliverstov, 2009) (Fig. 1a). The Avachinsky transform fault traces the boundary between the Eastern volcanic belt with the accretions of variously aged terranes in the north (Lander & Shapiro, 2007; Levashova et al., 2000; Tsukanov et al., 2014) and a long-lived island arc in Southern Kamchatka (Avdeiko et al., 2006). The Avachinsky transform fault is observed on the continental slope (Popruzhenko & Zubin, 1997), and in general, such deep transform faults can be considered as a boundary between variously aged slabs. The ages of the subducting Pacific slab are 87–92 Ma under the Eastern volcanic belt; under Southern Kamchatka, they are 103–105 Ma (Gorbatov et al., 1997) and 89–92 Ma (Eastern volcanic belt), 100–105 Ma (Southern Kamchatka) according to Syracuse and Abers (2006) (Fig. 1a). On the surface, the MPZ is detected by a large fracture zone, which is orthogonal to the present location of the subduction zone (Kozhurin et al., 2008) (Fig. 1b), and in seismic data, layers under the MPZ possess a low-velocity anomaly (Gontovaya et al., 2010). At least four regional faults are recognized on the surface (Geological map of the Russian Federation, 2000) (Fig. 1b, Suppl. 3). Based on geophysical observations, the upper crust of the MPZ is fractured by numerous individual ruptures zones (Nurmukhamedov & Sidorov, 2019; Sheimovich & Sidorov, 2000), forming basement heterogeneity (Moroz & Gontovaya, 2018). A regular geodetic network in the MPZ shows super-intensive fault movements, which also suggest active fault systems (Churikov & Kuzmin, 1998).

The origin of the prominent MPZ is debated. Based on geological mapping, the anomaly area with its arc-perpendicular-oriented geological formations and faults of the MPZ were first described in the complete monograph *Geology of the USSR* (1967). Kozhurin and Zelenin (2017), based on seismic sounding (Seliverstov, 1998), concluded that the Avachinsky, Kronotsky, and Kamchatsky bays originated by evolved synsedimentary processes and rapid submergence of the continental slope. The formation of the MPZ began in the Cenozoic (Shatser, 1987) to Late Miocene-Pliocene (Aprelkov et al., 1999; Dmitriev & Ezhov, 1977). Evolving

extensional, compressional, then strike-slip deformation along the MPZ has resulted in the formation of the arc-perpendicular graben-like structure filled with hundreds of meters of sediment derived from wide areas of Kamchatka (Geological map of the Russian Federation, 2000; Sheimovich & Sidorov, 2000). The Avacha Gulf is located in the MPZ and, according to Aprelkov and Svyatlovsky (1989), has a tectonic origin. The area where it connects with the Sredinny Range (Fig. 1) has resulted in recent tectonic exhumation of high-grade amphibolites to granulate Ganal metasediments, representing the basement of the arc with ages of 18–80 Ma (Bindeman et al., 2002). Geophysical researchers using converted-wave seismic exploration and magnetotelluric sounding suggest fragmentations of the crust and intrusions of magmatic bodies in various depths inside the MPZ (Nurmukhamedov & Sidorov, 2019). High heat flow (~ 80 mVt/m^2) was measured in the MPZ, while that in the surrounding area was 40–60 mVt/m^2 (Sugrobov & Yanovsky, 1991). The finding of alkalic and sub-alkalic rock in the frontal zone of the MPZ enabled some researchers to suggest an unusual subduction origin of the Miocene magmas (Balyev et al., 1984; Mitichkin et al., 1998; Sheimovich et al., 2005).

2.2. Volcanism in the MPZ

Volcanism in the MPZ occurs in two types: parasitic cones on the slopes of associated polygenetic stratovolcanoes, and numerous independent monogenetic cinder cones and extrusive domes (Figs. 2b, 3d) (Supplementary file 1). Stratovolcanoes include Koryaksky and Avachinsky volcanoes with known historic eruptions and Kozelsky and Vilyuchinsky volcanoes without known historic eruptions (Fig. 5). Geographically, most of the MPZ cinder cones are concentrated in the Paratunka and Bolshoy Vilyui river valleys (Figs. 1b, 2a, 3). Monogenetic cinder cones mark the location of long-lived faults of the MPZ (Favorskaya et al., 1965). The basaltic cinder cones are localized in the boundaries of silicic granitic intrusions, and fragments from these rock units are commonly entrapped within lava flows (Aprelkov & Borzova, 1963). Monogenic cinder cones in the valley of the
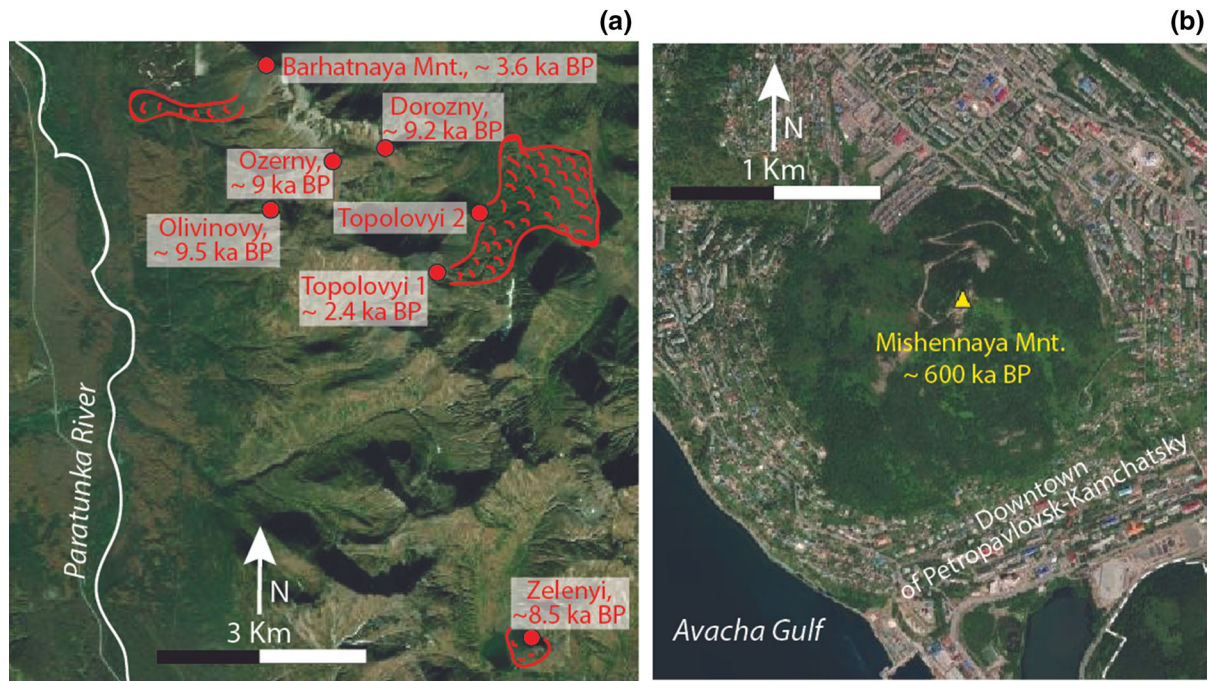
Figure 2
Satellite photos of the long-lived rupture zone with variously aged monogenetic cinder cones (**a**) and an extrusive dome (**b**). Locations of cinder cones and lava flows and ages are shown according to Dirksen (2009) and Geological map of the Russian Federation (2000)

Paratunka River were formed in two stages: 8–10 ka BP and 2.4–3.6 ka BP, based on tephrochronology (Dirksen, 2009). Erupted volumes of pyroclastic materials in the Early Holocene are $\sim$ 0.08 km^3 and $\sim$ 0.065 km^3 in the Late Holocene, based on studies of tephra distributions (Dirksen, 2009). In the southern part of the Avacha Gulf, there is a basaltic cinder cone forming an isolated island near Vilyuchinsk (Figs. 1, 2c). Its edifice volume projected to the sea floor is less than 3–4 km^3 (Dubik & Ogorodov, 1970). Most cinder cones on the north of the Avacha Gulf are parasitic cones of Koryaksky and Avachinsky volcanoes (Fig. 1). These cinder cones are located mainly on the regional fault (Fig. 1b). This regional fault is a margin of the Avachinsky graben (Figs. 1c, 13) and is well detected by geophysical data (Nurmukhamedov & Sidorov, 2019), basement heterogeneity (Sheimovich & Sidorov, 2000), and geological observations (Aprelkov et al., 1999; Geological map of the Russian Federation, 2000) (Suppl. 3).

Major extrusive domes (defined here as being predominantly made of viscous and blocky lava and not scoria) of the MPZ are localized in the north. One of the best examples is Mount Mishennaya (Figs. 2b, 3d). It is an extrusive dome with a basement diameter of $\sim$ 1 $\times$ 2 km (Sheimovich et al., 2007). It is a landmark hill with 385 m in altitude in downtown Petropavlovsk-Kamchatsky with a viewpoint and TV station, while its slopes are covered with residential and government buildings (Fig. 2d). The areal extent of the Mishennaya dome was estimated as 0.3 km^2 (Grib, 1985). The exposed thickness of andesitic rocks is 50–70 m on the northern slope of the cone, the flanks are covered with sedimentary rock of the Late Cretaceous Nikolskaya Suite (Sheimovich et al., 2007), with xenoliths of sedimentary rocks present in the base of the intrusion (Grib, 1985). The sedimentary rocks are presented by siliceous deposits, tuffs, and silts (Geological map of the Russian Federation, 2000). The age of the Mount Mishennaya according to fission-track analyses is 700 $\pm$ 200 ka (Geological map of the Russian Federation, 2000), and

600 ± 200 ka was obtained by K–Ar dating of hornblendes (Sheimovich et al., 2007). All other extrusive domes north of the MPZ are re-covered by debris avalanches of the Avachinsky volcano, which occurred ∼ 30 ka BP (Ponomareva et al., 2006). These andesitic extrusive domes, similar to Mount Mishennaya, were determined by geophysical methods and drill cores (Dmitriev & Ezhov, 1977; Geological map of the Russian Federation, 2000; Svyatlovsky, 1956). According to the Geological map of the Russian Federation (2000), the ages of their formations range from 10 to 110 ka BP, as determined by their geological relationship with surrounding rocks. Because extrusive domes are particularly visible in the area covered by volcanic debris avalanche deposits from Avachinsky volcano (∼ 30 ka BP formation according to Ponomareva et al., 2006), their age estimates are older than Holocene. A massive extrusive dome was also identified under the water on the north part of the Avacha Gulf based on bathymetry and geophysical investigations (Dmitriev & Ezhov, 1977). We therefore suggest a simple compilation of existing data for domes similar to Mount Mishennaya to identify their widespread abundance, requiring dedicated effort to determine their age, mode of emplacement and composition, as well as relation (or lack of it) to the other stratovolcanoes in the area, an attempt that we initiate in this study.

2.3. Spatial and Temporal Distributions of Monogenic Volcanism

The geochemical features of arc volcanoes in arc settings correlate to slab depths (Avdeiko et al., 2006; Duggen et al., 2007; Kimura & Yoshida, 2006 etc.). To check the role of the subducting slab in generating volcanism in the MPZ, we determined the pattern of variations in chemistry versus distance to the trench (Fig. 4). Stratovolcanoes are located ∼ 213–230 km from the trench, corresponding to depth to the subduction zone of 88 to 107 km for Kamchatka (Syracuse & Abers, 2006). Kozelsky and Vilyuchinsk volcanoes are frontal arc volcanoes, while Kozelsky (∼ 88 km slab depth), Avachinsky (∼ 94 km slab depth), and Koryaksky (∼ 107 km slab depth) volcanoes are tracing arc-perpendicular structures

(Fig. 4). Extrusive domes are mainly located in the northern part of the MPZ. Cinder cones are observed randomly located around 190 km and closer to the trench; most of the cinder cones are concentrated on the southern part of the MPZ. One cinder cone is located on the Khalaktyrsky beach, on the marked boundary of the Avachinsky graben (Fig. 1 b).

Geochronology for monogenetic cones is lacking, and thus there is an urgent need for radiogenic dating. Current knowledge is based on geological relationships and tephrochronology of the youngest cones. All stratovolcanoes in the MPZ started forming earlier than the Late Pleistocene and are currently considered active (Aprelkov and Borzynkova, 1963; Masurenkov et al., 1991). Based on tephrochronology, Vilchinsky and Kozelsky volcanoes had their last eruptions in the early Holocene (8–10 ka BP) (Holocene volcanism, 2020; Krasheninnikov et al., 2020). Since that time, those volcanoes have not had any volcanic activity. Koryaksky volcano was primarily active in the early Holocene when the Avachinsky volcano was quiet (Krasheninnikov et al., 2020). A phreatomagmatic eruption in 2009 AD on the western slope of Koryaksky volcano brought xenocrysts of sediments (minerals of rutiles, zircons, and corundums) filling the MPZ graben with zircon with ages ranging from 3400 Ma (oldest age for Kamchatka) to 1.8 Ma (Bindeman et al., 2016). The Avachinsky volcano had two stages of volcano activities in the Holocene. In the first stage (3.8–8 ka BP) it had rare but significant pyroclastic (pumice) eruptions; in the second stage (3.8 to present), it is characterized by more frequent pyroclastic explosions and lavas of basaltic andesitic magma compositions (Krasheninnikov et al., 2020). According to the Geological map of the Russian Federation (2000), monogenetic cinder cones present young postglacial volcanism, since the early Holocene. Noteworthy is the possible link between activities of stratovolcanoes and activation of monogenetic cinder cones (Fig. 5) (Aprelkov & Borzynova, 1963; Dirksen, 2009; Geological map of the Russian Federation, 2000; Global Volcanism Program, 2021; Holocene volcanism, 2020; Krasheninnikov et al., 2020; Masurenkov et al., 1991; Sheimovich et al., 2007). In the early Holocene, after the final eruptions of Kozelsky and Vilyuchinsky, monogenetic
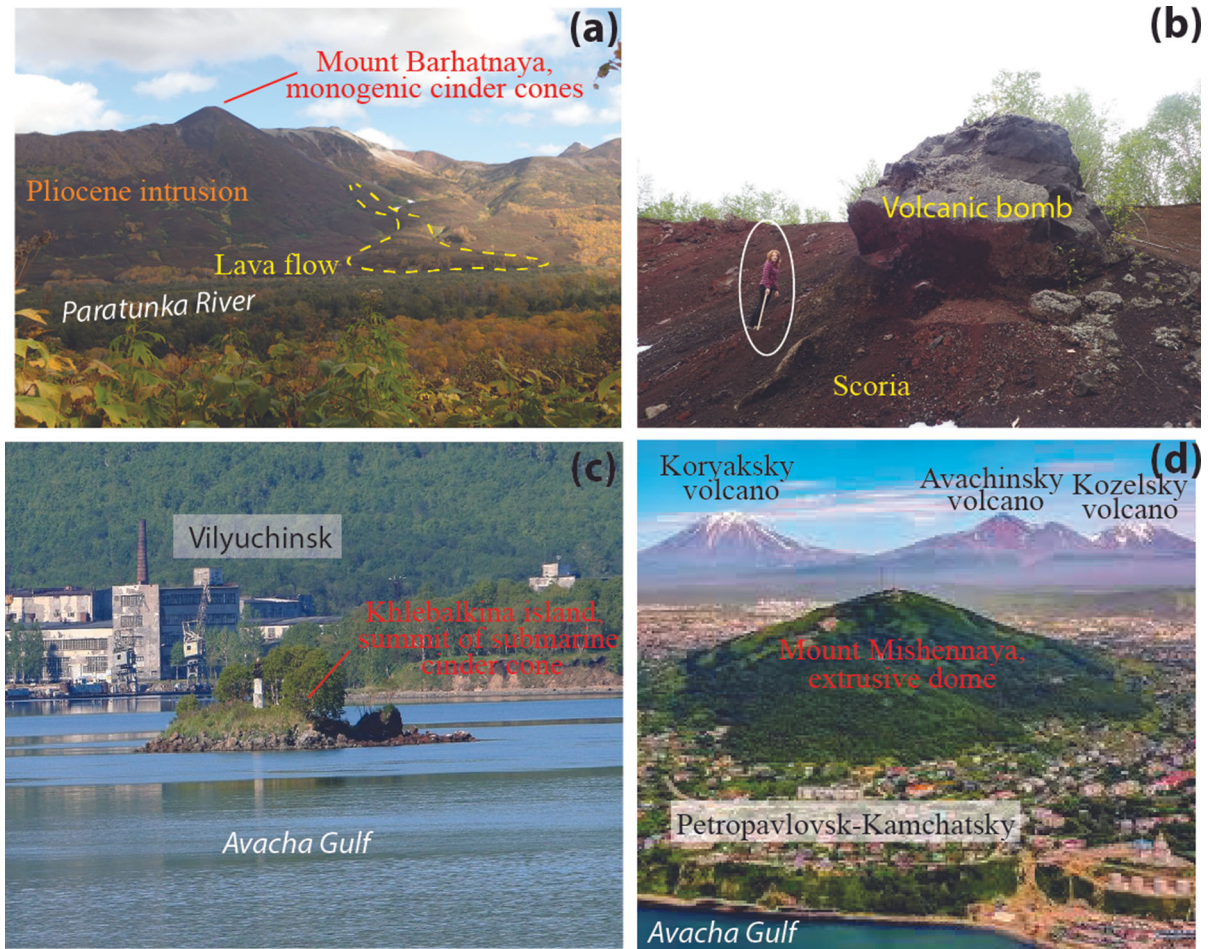
Figure 3
Photos of geological features associated with monogenetic volcanism in the MPZ. Locations of photos are in Fig. 1b; **a** cinder cone Barhatnaya in the valley of the Paratunka River; **b** cinder cone near Vilyuchinsk; **c** Khlebalkina Isl. is a summit of cinder cone of Avacha Gulf. Photo from www.press-toff.livejournal.com; **d** extrusive dome Mishennaya in the centre of Petropavlovsk-Kamchatsky. Photo from www.instazu.com

volcanism started to form. Since 3.8 ka BP, the focus of magmatic activity has shifted to the plumbing system of Avachinsky volcano, coincident with another activation of monogenetic volcanism (Fig. 5).

3. Samples and Analytical Methods

In this study, we collected 33 samples of Pleistocene-Holocene magmatic rocks. The sampling localities are shown in Fig. 1 and listed in Supplementary file 2. These include lava flows, bombs, and lapilli of monogenetic cinder cones (Fig. 3a, b, c) and fully crystalline andesites of the Mishennaya extrusive dome (Fig. 3d). Thin sections were prepared and examined under an Olympus BX51 polarizing microscope.

The whole-rock chemistry was determined by X-ray fluorescence (XRF) on an Axios^{mAX} vacuum wavelength dispersive spectrometer (Malvern PANalytical, Netherlands) at the Analytical Center, Institute of Geology of Ore Deposits, Petrography, Mineralogy and Geochemistry RAS (IGEM), Moscow. The measurement accuracy was controlled by international standard samples BCR-2 and BIR-1.
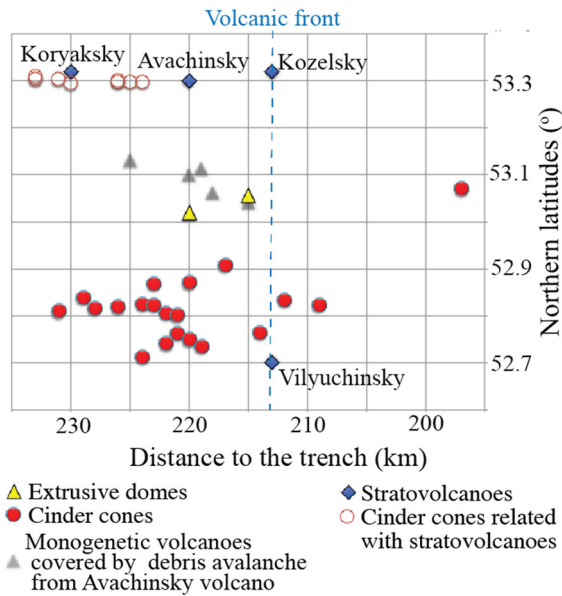
Figure 4

The geodynamic setting of the Holocene volcanoes in the MPZ in correlation to the distance to the trench. According to the Geological map of the Russian Federation (2000), positions of the cones are shown locations of the submarine cones in the Avacha Gulf by Dmitriev and Ezhov (1977). The blue dotted line is the hypothetical line of the volcanic front

the Vinogradov Institute of Geochemistry, Irkutsk, Russia. The analytical uncertainties were estimated from the systematic analysis of the BHVO-2 and AGV-2 rocks and calculated as less than 10%.

The high-precision MC-ICP-MS method (Rekhämper and Halliday, 1998) was used in this study for analysis of Pb isotope compositions in volcanic rocks, using the approach described in detail (Chernyshev et al., 2007). Analyses of Pb isotope ratios were carried out on a NEPTUNE mass spectrometer (Thermo Scientific, Germany) at the Laboratory of Isotope Geochemistry and Geochronology IGEM. For analysis, 0.04–0.06 g of the whole rock powder was taken. Samples were dissolved in a mixture of $HNO_3 + HF$ (1:3) for 2 days at 140 °C. Subsequently, the solution was evaporated to dry salts. Separation of Pb from major and trace rock elements was carried out using a one-step scheme with HBr medium in a chromatographic microcolumn (0.1 cm^3) filled with anion exchange resin AG 1-X8 (Chugaev et al., 2013). The blank laboratory contribution for Pb did not exceed 0.1 ng. Before isotope analysis, the Pb solutions (3% HNO_3) were preliminarily traced by Tl. Mass-bias correction for the measured Pb isotope ratios was performed using the reference ratio $^{205}Tl/^{203}Tl = 2.3889 \pm 1$ employing an exponential law. Precision and accuracy of the results were monitored by systematic analyses of the SRM 981 and referenced andesite

The analytical uncertainty was approximately 5% for the element whose content in the samples was no higher than 0.5 wt%. The trace element compositions were analysed via inductively coupled plasma mass spectrometry (ICP-MS), using the NexION 300D at
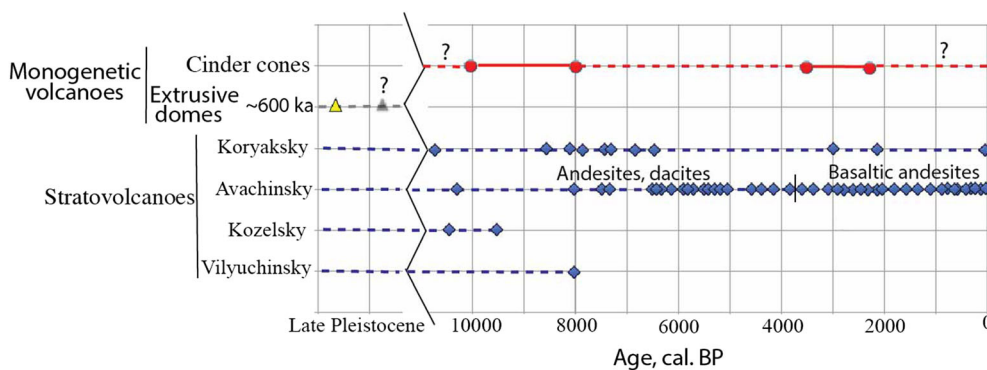

Figure 5

Temporal variations in monogenetic volcanoes and stratovolcanoes in the MPZ are based on data from Aprelkov and Borzynova (1963), Dirksen (2009), Geological map of the Russian Federation (2000), Global Volcanism Program (2021), Holocene volcanism (2020), Krasheninnikov et al. (2020), Masurenkov et al. (1991), and Sheimovich et al. (2007). Symbols show absolute dating of eruptions. The dotted line is the time of activations. Symbols are the same as in Fig. 3
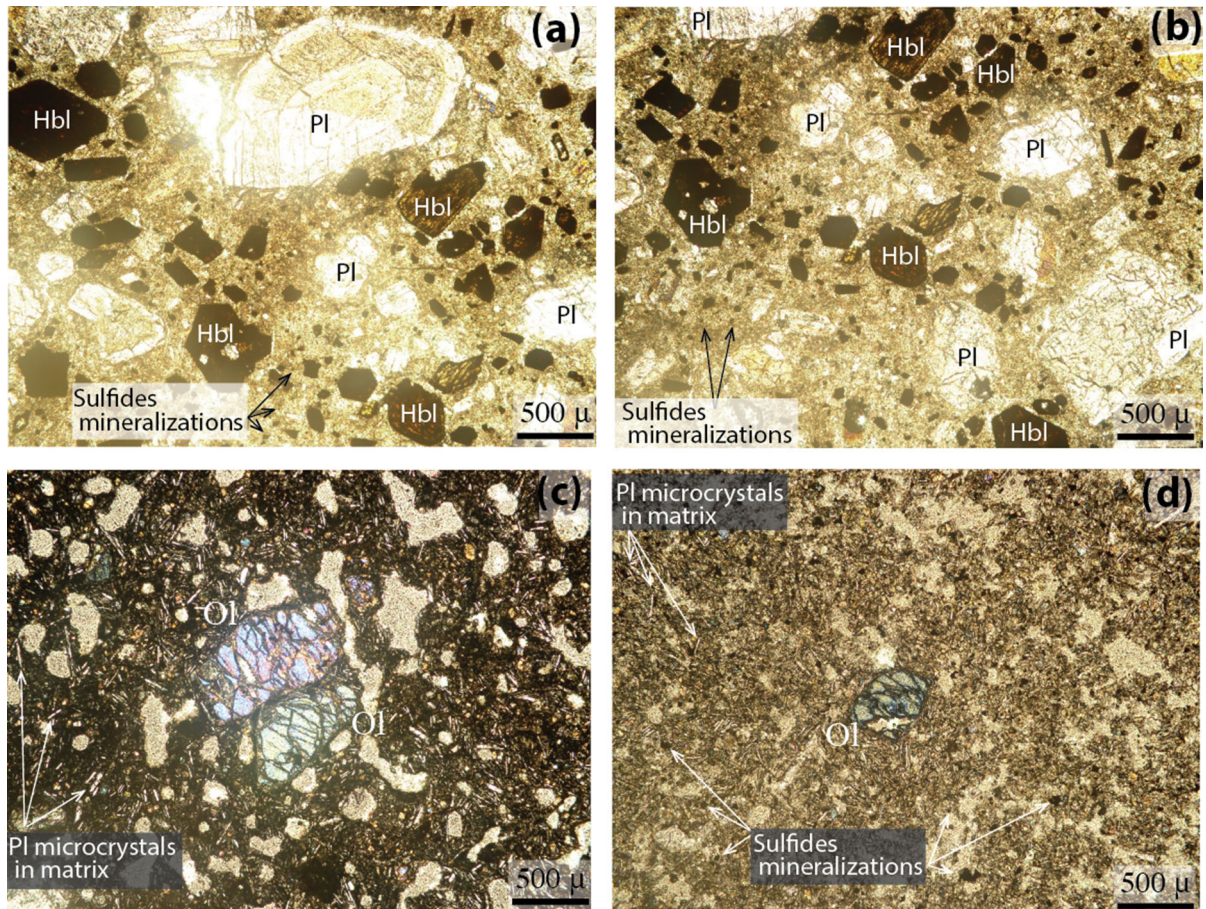
Figure 6
Thin sections of Hbl andesites of extrusive dome Mishennaya Mount (**a**, **b**) and Ol-bearing basaltic andesites of the monogenetic cones (**c**, **d**)

sample AGV-2. In a series of parallel analyses ($n = 4$), the average value of Pb isotope ratios for AGV-2 were $^{206}Pb/^{204}Pb = 18.871 \pm 5$; $^{207}Pb/^{204}Pb = 15.621 \pm 4$; and $^{208}Pb/^{204}Pb = 38.548 \pm 10$. The total error ($\pm$ 2 SD) of analysis for Pb did not exceed $\pm$ 0.03%.

The Nd–Sr isotopic ratios studies were carried out using a Sector 54 mass spectrometer (Micromass), using a multi-dynamic mode routine at the Laboratory of Isotope Geochemistry and Geochronology IGEM (Larionova et al., 2007). The effects of mass fractionation were corrected using an exponential law, via normalizing to $^{86}Sr/^{88}Sr = 0.1194$ and $^{146}Nd/^{144}Nd = 0.7219$. The $^{87}Sr/^{86}Sr$ ratio of the SRM-987 Sr standard measured during the period of the analytical session averaged 0.710242 ± 11 ($\pm$ 2

SD, $N = 10$). The mean of the LaJolla Nd standard runs during the period of data collection was for $^{143}Nd/^{144}Nd = 0.511850 \pm 9$ ($\pm$ 2SD, $N = 10$).

4. Results

4.1. Petrography and Mineral Assemblages

The extrusive dome of Mount Mishennaya has a fine-grained, phenocryst-rich texture, and 40–50% of the rocks are made of phenocrysts of plagioclase (Pl) and hornblende (Hbl) in the fully crystalline form, not vesicular rocks. Pl as Hbl have two generations with various crystal sizes. Generation A of Pl with ~ 1000 μm and Hbl ~ 500 μm have regular shapes, with some Pl characterized by honeycomb structures.
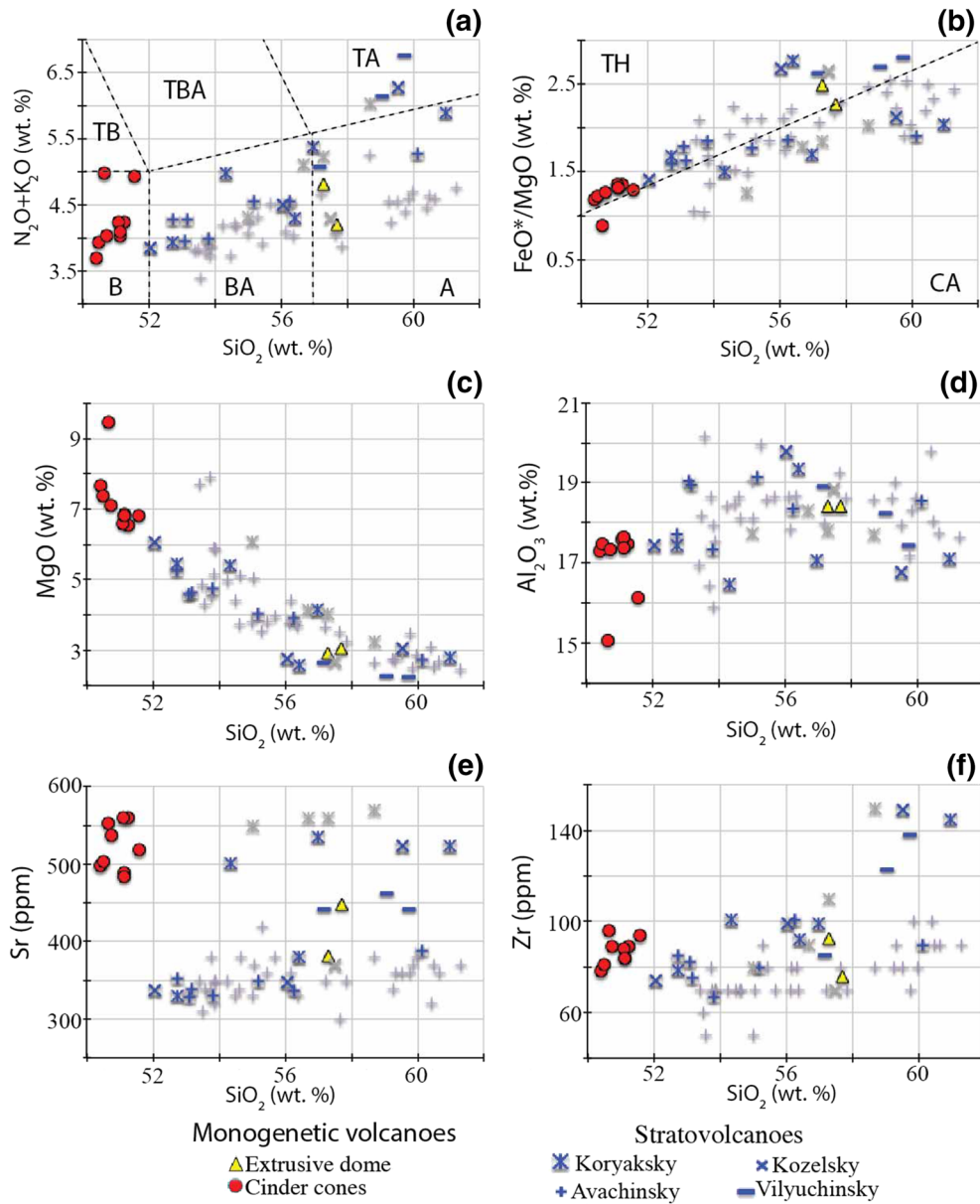
Figure 7
Silica variation diagrams with significant oxides and trace elements. Abbreviations in the total alkali–silica (TAS) diagram (**a**) indicate standard fields of rock compositions are basalts (B), basaltic andesites (BA), andesites (A), trachybasalts (TB), trachybasaltic andesites (TBA), and trachyandesites (TA). Discrimination lines on tholeiitic (TH) and calc-alkaline series on the diagram (**b**) are according to Miyashiro (1974). Grey symbols are tephra compositions from Koryaksky, Avachinsky, and Kozelsky volcanoes (Krasheninnikov et al., 2020)

The generation B phenocryst assemblage is characterized by smaller sizes of crystals of Pls $\sim$ 500 μm and Hbls $\sim$ 100–200 μm with stronger zoning crystals, but euhedral crystal shape. Groundmass contains sulfide crystals (Fig. 6a, b).

Samples of cinder cones near the Vilyuchinsk volcano (MPDZ-12a) have aphanitic, sometimes porphyritic, textures (Fig. 5c, d) with an olivine-phyric (Ol $\sim$ 10%) texture. The groundmass is vesicular with $\sim$ 30% of the bubbles in basaltic
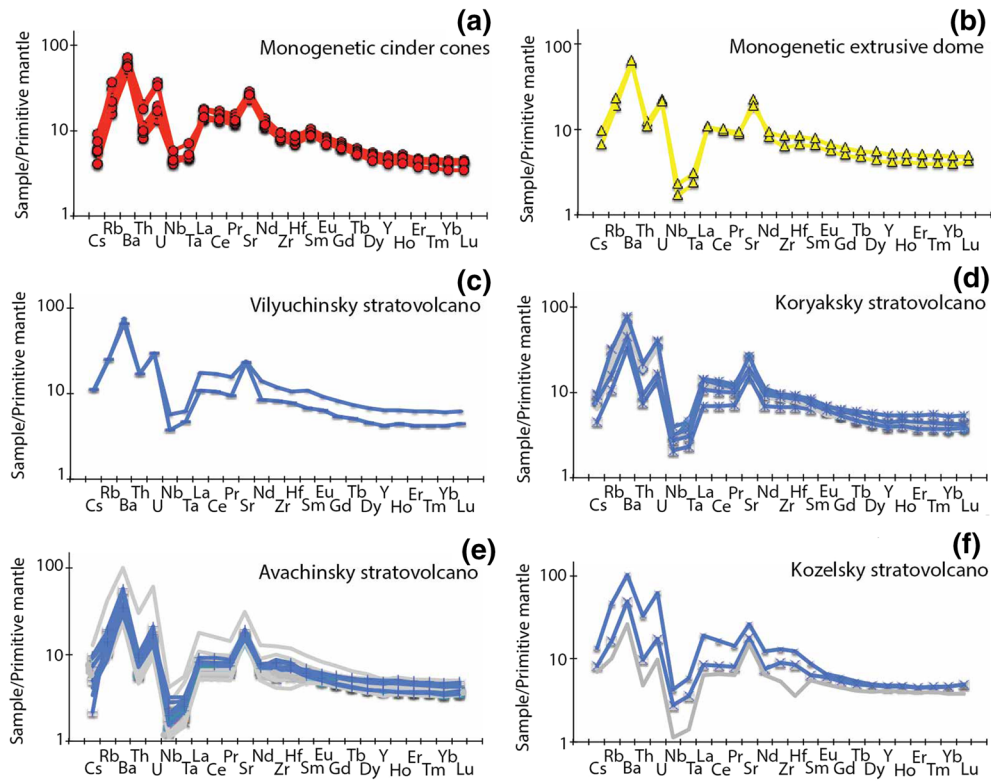
Figure 8
Primitive mantle-normalized multi-element concentration diagrams. Trace element concentrations of the primitive mantle are taken from Sun and McDonough (1989). Grey symbols are tephra compositions from Koryaksky, Avachinsky, and Kozelsky volcanoes (Krasheninnikov et al., 2020)

glass. The absence of microcrystals in the matrix could be interpreted as rapidly crystallized lava on or near the surface. Some of the thin sections were observed to be Pl microlites in the groundmass (Fig. 6c, d).

4.2. Geochemistry and Pb–Sr–Nd Isotopic Ratios

4.2.1 Major and Trace Elements

Harker diagrams are presented in Fig. 7. Monogenetic cinder cones are basalts (50–52 wt% SiO_2) with low alkali content (3.5–5 wt% $Na_2O + K_2O$, 3.3–3.8 N_2O/K_2O). The extrusive dome of Mishennaya Mount is andesitic with 57–58 wt% SiO_2, 4–4.8 wt% $Na_2O + K_2O$, and 4.4–5.2 N_2O/K_2O (Fig. 7a). Using Miyashiro's FeO/MgO diagram, almost all monogenetic cones belong to the tholeiitic series, same as the extrusive dome (Fig. 7b). A high MgO

($\sim$ 6.5 wt%) value characterizes primitive magma of monogenetic cinder cones, while the extrusive dome has lower MgO content ($\sim$ 3 wt%) (Fig. 6c). Al_2O_3 varies from 15 to 17 wt% for monogenetic cones and $\sim$ 18% for the extrusive dome (Fig. 6d). Trace element variations, especially Sr, have the highest (> 450 ppm) values for basaltic monogenetic cinder cones and the lowest ($\sim$ 40 ppm) for more differentiated extrusive domes, as explained by plagioclase fractionation (Fig. 7e). Zr variations are relatively low (70–100 ppm) and nearly the same for cinder cones and extrusive domes (Fig. 7f).

Trace element patterns of MPZ rocks normalized to primitive mantle have enriched large-ion lithophile elements (LILE) (Rb, Ba and Sr), Th, and depleted high-field-strength elements (HFSE) (Nb, Ta) (Fig. 8), a typical pattern for island arc origin. Chondrite-normalized patterns of rare earth elements are presented in Fig. 9. The heavy rare earth elements
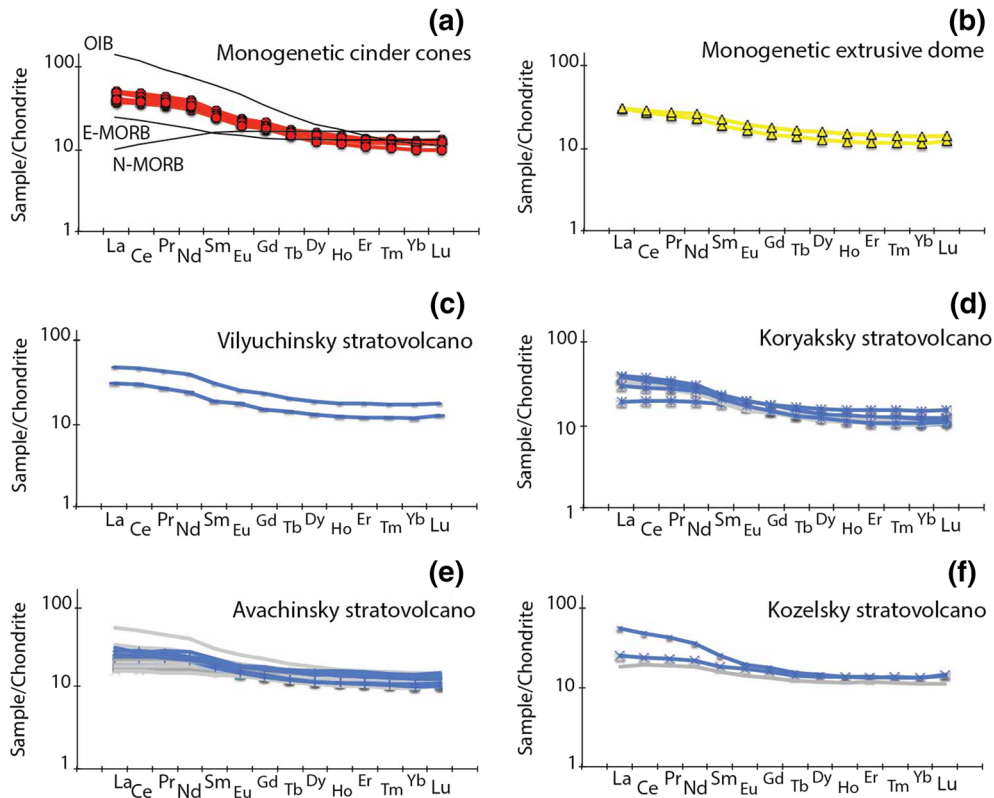
Figure 9
Chondrite-normalized trace element diagrams. Enriched mid-ocean ridge basalts (E-MORB), depleted mid-ocean ridge basalts (N-MORB), and ocean–island basalts (OIB) are according to Sun and McDonough (1989). Grey symbols are tephra compositions from Koryaksky, Avachinsky, and Kozelsky volcanoes (Krasheninnikov et al., 2020)

(REE) with smaller ionic radius (e.g. Lu, Yb, Tm, Er) are nearly the same for all the rocks. There is a slight enrichment of La, Ce, Pr, Nd, and Sm for monogenetic cinder cones (Fig. 9a) and Koryaksky (Fig. 9d) and Vilyuchinsky (Fig. 9c) stratovolcanoes.

4.2.2 Pb–Sr–Nd Isotopes

The Sr–Nd isotopic ratios vary within narrow ranges (Fig. 10a). The monogenetic extrusive dome shows similar variations as rocks from Southern Kamchatka and the Eastern volcanic belt. However, monogenetic cinder cones have lower $^{143}Nd/^{144}Nd$ isotopic ratios (0.512959–0.512999) and variable $^{87}Sr/^{86}Sr$ isotopic ratios (0.703356–0.703451). The lower $^{143}Nd/^{144}Nd$ isotopic ratios could be interpreted as an indicator for a slightly enriched mantle component, e.g. E-MORB (Fig. 10a), or lower crustal assimilation. The lead

isotopic composition is similar to rocks from the Eastern volcanic belt and Southern Kamchatka (Fig. 10b). The coefficient of variations for Pb isotopic ratios estimated as a ν (%) are $\nu_{6/4} = 0.29$, $\nu_{7/4} = 0.14$, and $\nu_{8/4} = 0.20\%$. The variations are relatively small, but are almost an order higher than the analytical error. Variously aged rocks could not explain the observed heterogeneity of the Pb isotopic composition in the rocks. Thus, estimated lead isotopic ratios reflect the primary process of magma genesis (Lustrino et al., 2010; Oyan et al., 2017). Kamchatkan altered oceanic crust (K-AOC) and Kamchatkan subducted sediments (KSSC) as determined by Duggen et al. (2007) were compared with rocks from the MPZ (Fig. 10b). Variations in lead isotopes suggest that monogenetic volcanoes have similar variations with polygenic stratovolcanoes. However, the ranges of variations in monogenetic
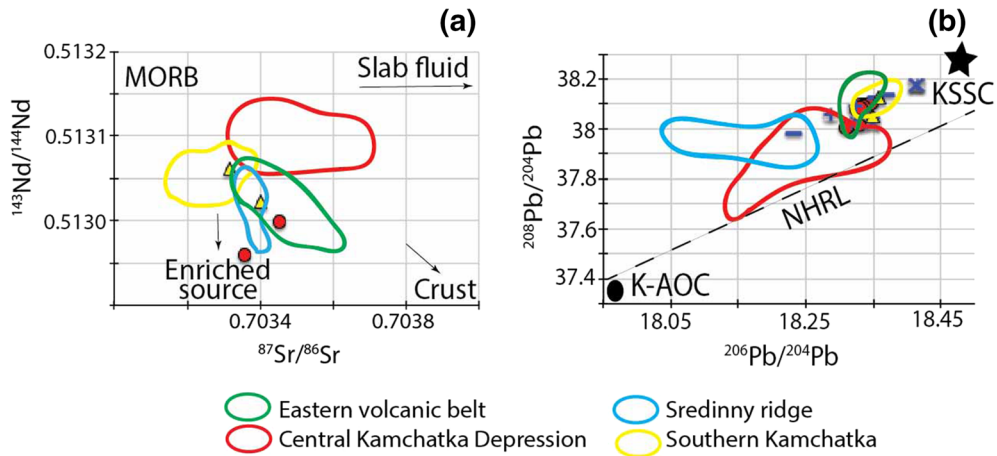
Figure 10
Sr–Nd (**a**) and Pb isotope diagrams (**b**) show monogenetic and polygenetic volcanoes. Symbols are the same as in Fig. 7. The dashed line is the Northern Hemisphere Reference Line (NHRL) (Hart, 1984). The star is the Kamchatka subduction sediment column (KSSC). The black circle is Kamchatkan altered oceanic crust (K-AOC) according to Duggen et al., (2007). Isotope variations in the Eastern volcanic belt, Sredinny ridge, and Central Kamchatkan Depression are based on Churikova et al. (2001). Southern Kamchatka isotope variations are preset by Duggen et al. (2007)
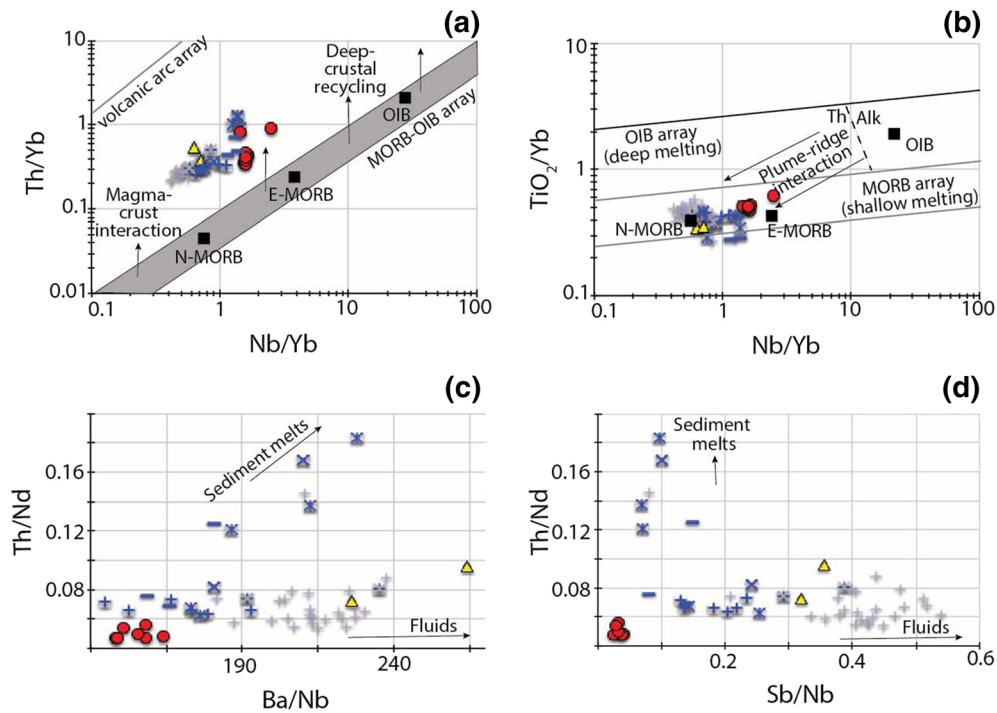

Figure 11
Ratios of trace element variations. Discrimination lines on a-b patterns are according to Pearce (2008). Symbols are the same as in Fig. 7
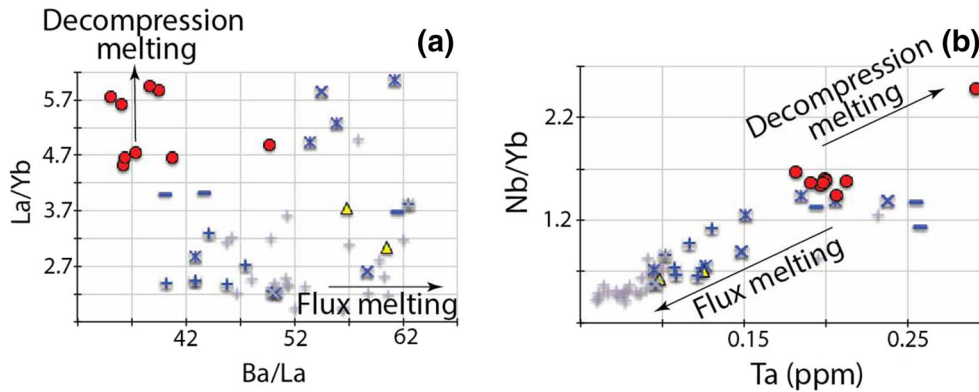
Figure 12
The Ba/La versus La/Yb (**a**) and Nb/Yb versus Ta (**b**) diagrams identify the main melting process in the mantle wedge

volcanoes are narrow ($^{206}Pb/^{204}Pb \sim 18.30\text{–}18.45$, $^{208}Pb/^{207}Pb \sim 38.00\text{–}38.12$) as compared to polygenetic stratovolcanoes ($^{206}Pb/^{204}Pb \sim 18.23\text{–}18.41$, $^{208}Pb/^{207}Pb \sim 37.98\text{–}38.17$). Polygenetic stratovolcanoes, especially the Koryaksky volcano, show greater variations and trends extending to KSSC (Fig. 10b).

5. Discussion

5.1. Geochemical Insights into the Origin of Monogenetic Volcanism

Fluid-immobile HFSE are good indicators of the extent of the melting process in the mantle wedge, as well as the degree of its prior melting/enrichment (Duggen et al., 2007). The largest Nb–Ta minimums on spider diagrams of the monogenetic cinder cones indicate some differences in magma origin from the polygenetic stratovolcanoes (Fig. 8a). The highest Nb/Yb and Ti/Yb ratios on Pearce diagrams (Fig. 11a, b) indicate an enriched mantle source represented by E-MORB mantle. In contrast, extrusive dome and stratovolcanoes are derived from an N-MORB type of mantle. This observation also correlates with Sr–Nd isotopic ratios (Fig. 10a, b), where monogenetic cinder cones have lower Nd isotopic ratios, in contrast to the extrusive dome and stratovolcano trends encompassing the Southern Kamchatka, Sredinny ridge, and Eastern volcanic belt. The monogenetic cinder cones are also

characterized by the highest content of incompatible elements (e.g. K_2O, Zr, and Sr) (Fig. 7). Variations in light rare earth elements (LREE) with the largest ionic radius (La, Ce, Pr, and Nd) on the chondrite-normalized patterns could be interpreted as reflecting the various degrees of partial melting in the wedge. However, there is no correlation between those elements, and isotopic variations in Pb isotopes are not observed (Fig. 10d), suggesting that subduction sediment is not affecting LREE. As a rule, in a subduction zone setting, the degree of partial melting decreases from the front to the rear arc zone (Churikova et al., 2001; Kimura & Yoshida, 2006). Confirming this, the Koryaksky stratovolcano, which is located in the rear arc, is characterized by higher content of rare earth elements (Fig. 9d). At the same time, the front arc Avachinsky and Kozelsky volcanoes have significant variations in LREE La, Ce, and Sm (Fig. 9e, f), signifying diverse regimes of magma genesis. These data cannot be explained solely by different degrees of partial melting of a uniform mantle. In order to check the melting regime, we used ratios of La/Yb, Ba/La, and Nb/Yb (Fig. 12). Maximum La/Yb correlates with a minimum Ba/La ratio for monogenetic volcanoes (Fig. 12a), which is different from polygenetic volcanoes. Together, changes in Nb/Ta and Ta and the highest content indicate that decompression melting plays a predominant role for monogenetic volcanoes (Fig. 12b). Variations in fluid-immobile (Fig. 13a, b) and mobile elements (Fig. 13c, d) versus distance to trench do
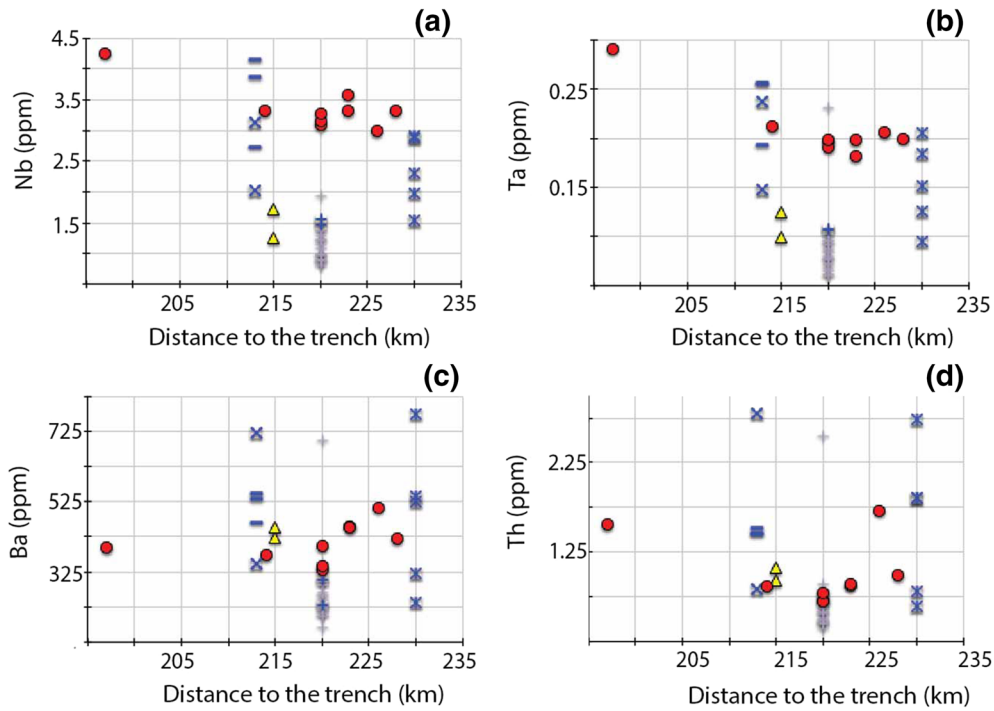
Figure 13
Variations in fluid-immobile (**a**, **b**) and fluid-mobile elements (**c**, **d**) versus distance to the trench. Symbols as in Fig. 7

not show classical across-arc variations. From the front to rear zone, the content of Nb and Ta decreases (Fig. 13a, b), but the content of Ba and Th stays (Fig. 13c, d) nearly the same. It is important to note that Avachinsky and Koryaksky volcanoes are characterized by classical across-arc variations with increasing content of LREE and HFSE from the front to rear arc zone. However, Kozelsky and Vilyuchinsky volcanoes do not follow this trend. A possible explanation is the age of formation, in that the volcanoes are much older than other stratovolcanoes. During the historical observations (since ~ 1700 AD), they have had no eruptions, and the last eruptions were in the Early Holocene (Fig. 5). Consequently, the degree of partial melting of Pleistocene activation of the Kozelsky and Vilyuchinsky volcanoes was much lower than the Holocene rocks of the Avachinsky and Koryaksky volcanoes. The high content of Nb, Ta, and other fluid-immobile elements of frontal volcanoes would be explained by a smaller degree of partial melting in the mantle wedge.

Ratios of fluid-mobile elements and Pb isotope data were used to infer slab inputs under Southern Kamchatka (Duggen et al., 2007) and more recently of Koryaksky, Avachinsky, and Kozelsky stratovolcanoes (Krasheninnikov et al., 2020). The highest values of Th/Nd (Fig. 11c, d) correlating with $^{206}Pb/^{204}Pb$ ratios (Fig. 10c, d) suggest an increased role of sediment melts from the slab under the rear arc Koryaksky stratovolcano. In contrary, the frontal volcanoes, e.g. Avachinsky, Kozelsky, and Mishennaya extrusive domes, have higher Ba/Nb and Sb/Nb ratios (Fig. 11c, d). These indicate significant input of the fluid-derived slab component, e.g. slab dehydration. Monogenetic cinder cones have remarkably lower fluid-mobile ratios than other volcanic rocks in the MPZ (Fig. 11c, d). Thus, contributions of the slab components to their genesis are minimum.

To estimate the depth of magma crystallization, pressure and temperatures conditions were obtained using the Helz and Thornber (1987) glass (or liquid) thermometer and Putirka (2008) glass (silica activity) barometer (Fig. 14), and these petrological estimates
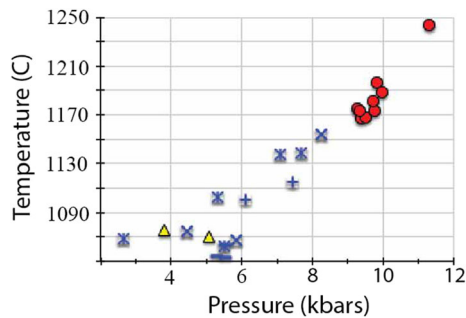
Figure 14

Pressure and temperature conditions for magma crystallization. Calculations are based on a glass thermometer by Helz and Thornber (1987) and glass barometer by Putirka (2008). Symbols are the same as in Fig. 6
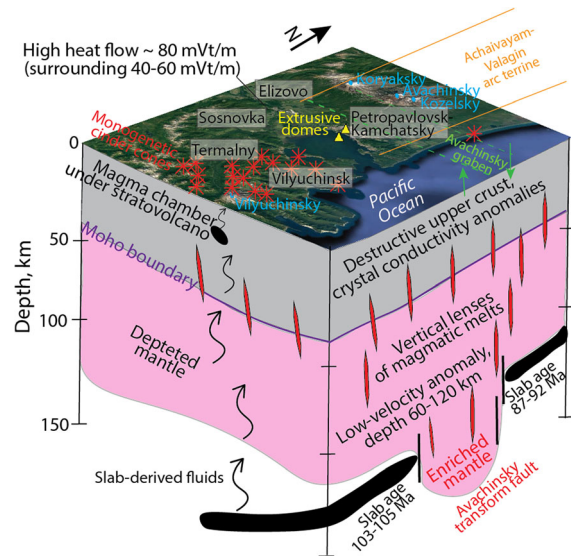

Figure 15

Schematic model of the generation of monogenetic volcanism in the MPZ based on a combination of geophysical, geochemical, and geological data. The position of the Achaivayam-Valagin arc terrane in the basement of the north part of the MPZ is shown according to Chekhovich and Sukhov (2006). Crustal anomalies and crustal structure are according to Aprelkov et al. (1999), Loginov and Gontovaya (2020), Nurmukhamedov and Sidorov (2019), and Sheimovich and Sidorov (2000), heat flow (Sugrobov & Yanovsky, 1991), deep low-velocity anomaly (Gontovaya et al., 2010; Moroz & Gontovaya, 2018)

are correlated with geophysical observations. Based on mantle tomography, the depth of the magma chamber under Koryaksky volcano is $\sim$ 7 km, and there is a shallow magma reservoir at the Avachinsky volcano at $\sim$ 2 km depth below the surface (Bushenkova et al., 2019). Our petrological estimations are 1–8 kbar, and the depths of magma chambers of stratovolcanoes vary over a wide range of 3–21 km (Fig. 11). Parental magma of extrusive domes is estimated to reside at depths of 12–15 km (4–5 kbar); the country rocks at these depths are represented by the basaltic-metasedimentary basement of the Cretaceous Achaivayam-Valagin volcanic arc. Temperature estimations for stratocones and extrusive domes are 1050–1150 °C (Fig. 14). The deepest magma source zones are calculated for monogenetic cinder cones at 27–33 km (9–11 kbar) and also display the highest temperatures of $\sim$ 1160–1240 ° C. These estimates suggest that the basaltic magmas feeding monogenetic eruptions are coming directly from their storage conditions in the mantle or the Moho. These data show a reasonable correlation with depths of the high-electrical-conductivity anomaly in the MPZ (Moroz & Gontovaya, 2018) (Fig. 15). The absence of peripheral, shallow magma chambers in geophysical images suggests feeding of these deep reservoirs by regional faults (Fig. 1) that control the distribution of volcanism. Such faults were observed near the Vilyuchinsky volcano (Florensky & Bazanova, 1989; Sheimovich & Patoka, 2000).

5.2. Importance of Studying Monogenetic Volcanism for Society

The formation of monogenetic cinder cones in the MPZ is interesting not only for researchers but also important for local populations. The deep $\sim$ 30 km arc-perpendicular regional faults form the Avacha Gulf in the middle of Kamchatka's Pacific coast (Fig. 1, (Moroz & Gontovaya, 2003), which is the main transport gateway to Kamchatka. According to the Federal State Statistics Service (2020), most of the Kamchatkan populations live around the Avacha Gulf: Petropavlovsk-Kamchatsky ($\sim$ 180,000 people), Vilyuchinsk ($\sim$ 23,000 people) and Elizovo ($\sim$ 47,000 people) and smaller towns (Fig. 1). All these cities are located within the MPZ faults and potentially could be affected by eruptions of monogenetic volcanoes, as well as seismic activity along these faults.

Twenty-seven monogenetic volcanoes have been identified so far and studied in this report. Most of the cones are located in the southern part between latitudes 52.7° N and 52.9° N (Fig. 2), and thus the area has a potential for future monogenetic volcanic activity, requiring paying more attention to the MPZ. The government and scientists need to continue monitoring fault movements based on the existing and future geodetic networks and install seismic stations. These will help distinguish tectonic earthquakes along the fault and volcanically triggered earthquakes. Applying diverse geophysical methods, i.e. seismic, electromagnetic, and gravity, as well as ground-surface monitoring using InSAR, is necessary for better understanding the structure of the crust in the MPZ and detecting weak parts of fracture zones as is done in other parts of the world where populations live around seismic and volcanic hazards. In a parallel effort, geochemical and isotopic data on erupted products and microprobe analyses of phenocrysts should enable determination of conditions of magma crystallization in plumbing systems, magma differentiation in the crust, and, in particular, their volatile concentration relevant for explosive behaviour. Future studies are necessary to (1) identify new cones, especially the ones under sedimentary cover and under the Avacha Gulf, (2) date them using radiogenic methods, (3) predict the character and likelihood of future eruptions and their potential magnitude, duration, and impact, (4) identify gas release by these volcanoes and potential ash and tephra hazard, and (5) alert local populations for the likelihood of future eruption for the purpose of creating hazard maps and for the purpose of insurance.

Monogenetic volcanism formed during the Holocene (Supplementary file 1) also provides positive aspects to the population by creating recreational and touristic opportunities of vistas and isolated islands; these are currently utilized as a basement for lighthouses in the Avacha Gulf and for cell and radio/TV transmission stations (such as those on Mt. Mishennaya in downtown Petropavlovsk-Kamchatsky; Fig. 2). Many life-line infrastructures are associated with these volcanic features. Cinder cones on the coastline are quarried for road and construction material, recently used, for example, at fish processing plants. The Mount Mishennaya extrusive dome was quarried before 1990, and one monogenetic cinder cone near Vilyuchinsk is a large factory specializing in the development of gravels and sands.

The elevated grounds of local coastal cinder cones could provide good vertical escape shelter and routes for potential tsunamis. This is especially important in lights of recent understanding the paleotsunami record: 33 tsunamis were recorded on Khalaktyrsky beach (Pinegina et al., 2018) (Fig. 1) spanning the last $\sim$ 4200 years.

Geohydrothermal potential is another area of application. Numerous dikes and sills were observed at depths up to 7 km (Sheimovich & Sidorov, 2000). According to geophysical observations (Nurmukhamedov & Sidorov, 2019), the intrusive bodies intruded at the lower crust and did not reach the surface. Drilling cores at depths of 600–1500 m met with basic/intermediate compositions of intrusive bodies and were characterized by maximum water temperatures ($\sim$ 100 °C) (Chudaev et al., 2016). According to geochemical and stable isotopic variations, the hot spring along the Paratunka River is represented by heated meteoric water (Chudaev et al., 2000). Its circulation is responsible for the highest local heat flow ($\sim$ 80 mVt/m^2 according to Sugrobov & Yanovsky, 1991) observed in the MPZ.

5.3. The Correlation Between Tectonic Settings and Origins of Monogenetic Volcanoes

Heterogeneity of slabs controls magma genesis and their geochemical features (Bergal-Kuvikas et al., 2017; Churikova et al., 2001; Kimura & Youshida, 2006). Ridge–trench collision in the Chilean Patagonia formed a slab window and generated monogenetic cinder cones (Gutierrez et al., 2005). The active rifting in western Mexico was produced by Pacific plate heterogeneity on the boundary of the Rivera transform fault between the Cocos and Rivera plates (Ferrari et al., 2000). The lavas of monogenetic cinder cones surrounding the Bakening volcano in Kamchatka have signatures of an ocean–island basalt (OIB)-type enriched mantle source or slab component addition (Dorendorf et al., 2000). Intraplate monogenetic volcanoes in northern

New Zealand represent mantle upwelling linked to the long-term tectonic evolution of the Pacific-Australian Plate boundary beneath the New Zealand region (Smith et al., 2021). Delamination of the Neotethyan slab produces mafic monogenetic volcanoes in south-central Anatolia (Gall et al., 2021).

These worldwide examples demonstrate that spatial distribution of volcanism reflects the regional tectonic setting (Valentine & Connor, 2015). Monogenetic volcanism typically occurs in the extensional regime (Connor et al., 2000; Le Corvec et al., 2013; Nemeth, 2010). Geochemical data have shown that active extension, lithosphere rupture, and asthenospheric upwelling formed the monogenetic volcanoes in the Gulf of California (Calmus et al., 2011). In general, formation of monogenetic volcanoes is favoured in zones of high extension rate and/or low magma input (Alaniz-Alvarez et al., 1998; Takada, 1994). Magmatism can induce extension by injection of mafic magmas at the base of the crust and may cause buckling of the lithosphere because of the accumulation of low-density hot material (Yamasaki & Gernigon, 2009). On the surface, the numerous faults may form grabens in extension regimes (Marrett & Allmendingar, 1992; Nieto-Samaniego et al., 1999).

We have estimated that monogenetic cinder cones in the MPZ were formed by the enriched mantle source (low Nd isotopic ratios) (Fig. 10) with dominant decompression melting basalts having the highest Nb/Yb and La/Yb ratios (Fig. 12) without significant inputs of the slab's fluid components (the lowest Ba and Th content) (Fig. 11). The comparison with surrounding Kozelsky, Avachinsky, Koryaksky, and Vilyuchinsky stratovolcanoes supports this somewhat unusual origin of monogenetic volcanoes in the Kamchatkan subduction zone. A possible origin of melt coming from the enriched mantle source and decompression melting feeding monogenetic cinder cones is the Avachinsky transform fault. The slab windows, linking asthenosphere upwellings formed by subduction transforms faults and ridges, are observed in many other island arcs (e.g. Central America, Johnson & Thorkelson, 1997; North America, McCrory et al., 2009; Japan, Kinoshita, 1999). Kamchatka may not be an exception to other island arcs. Adakites and Nb-enriched basalts marked the

slab windows on the boundaries of the Kronotsky paleoarc accretion, e.g. in the MPZ (Avdeiko & Bergal-Kuvikas, 2015). Calculations of the pressure (9–11 kbar) and temperature (1160–1240 °C) (Fig. 14) conditions suggest magma residence of monogenetic cinder cones near the Moho boundary (Fig. 15). Accumulations of the low-density hot magmas could be causes of the extensional regime (Yamasaki & Gernigon, 2009). The Avachinsky graben and related monogenetic cinder cones mark the manifestation of this extension tectonic regime on the surface. Unfortunately, modern monitoring of the dynamic area by a geodetic network is not yet available. However, since mid-1999, increased seismicity and "superintensive fault movements" have been registered along the faults of the MPZ (Churikov & Kuzmin, 1998). In this way, the generation of monogenetic cinder cones in the MPZ correlates with an active extension tectonic setting, as observed at numerous arcs settings (Le Corvec et al., 2013).

6. Summary

This work draws attention to the spatial distribution and origin of monogenetic volcanism, most of the Holocene age, in the MPZ, inside or in proximity to major population centres in the Kamchatka Peninsula. The summary remarks of the presented research are as follows:

1. The combination of geological, geochemical, and geophysical data indicates that the high-electrical-conductivity anomaly in the crust (depths of 10–40 km according to Moroz and Gontovaya, 2018) and low-velocity anomaly in the uppermost mantle correlate with the potential sources of Holocene monogenetic volcanism on the boundary between variously aged slabs on the long-lived arc-perpendicular transform fault.
2. Trace element variations and isotopic data demonstrate that a relatively enriched mantle source with minimum inputs of the slab's components is required to generate monogenetic cinder cones. Their origin and chemical and isotopic composition are not so different from polygenic

stratocones of Avachinsky, Vilyuchinsky, and other volcanoes. However, the highest content of Nb/Yb, Ta, and La/Yb ratios indicates the domination of decompression melting in the genesis of monogenetic volcanoes.

3. Most monogenetic cinder cones trace linear arc-perpendicular rupture zones, and their magmas are determined to ascend rapidly from the lower crust. As some cones have ages from 9.2 to 2.4 ka (Dirksen, 2009), there were several stages of activations on these rupture zones. Given the relatively young Holocene age, this means that monogenetic cinder cones can still have an active magma plumbing system with geothermal potential.

4. As most of the population of Kamchatka lives close to these monogenetic cinder cones and extrusive domes, it is necessary to establish a continuous monitoring system using seismic data, ground deformation, and gas and water analysis to predict potential dangers of volcanic hazard and geothermal benefits from monogenetic volcanoes in the future.

Availability of data and material

The list of monogenic cinder cones (Supplementary file 1), their geochemical and isotopic measurements (Supplementary 2), and demonstration of the genesis of the long-lived transform fault under the MPZ (Supplementary 3) are available in Bergal-Kuvikas et al. (2021), "Monogenetic volcanism at Malko-Petropavlovsk zone of the transverse dislocation (Kamchatka)", Mendeley Data, V1, https://doi.org/10.17632/8d69jr8yjv.1 https://data.mendeley.com/datasets/8d69jr8yjv/draft?a=33739679-5dee-4b10-9d3f-ded4d55e79b8

Code availability

Not applicable.

Declarations

Conflict of interest The authors declare that they have no conflict of interest.

Publisher's Note Springer Nature remains neutral with regard to jurisdictional claims in published maps and institutional affiliations.

REFERENCES

Alaniz-Alvarez, S. A., Nieto-Samaniego, Á. F., & Ferrari, L. (1998). Effect of strain rate in the distribution of monogenetic and polygenetic volcanism in the Transmexican volcanic belt. *Geology, 26*(7), 591–594. https://doi.org/10.1130/0091-7613(1998)026%3c0591:EOSRIT%3e2.3.CO;2

Albert, H., Costa, F., & Martí, J. (2016). Years to weeks of seismic unrest and magmatic intrusions precede monogenetic eruptions. *Geology, 44*(3), 211–214. https://doi.org/10.1130/G37239.1

Andreev, A. A. (1993). Transform faults of the Earth's crust Northwestern Pacific. *Pacific Geology, 3*, 11–20. in Russian.

Aprelkov, S. E., & Borzova, G. P. (1963). Young volcanic structures around Avacha bay. *Questions of Geography of Kamchatka, 1*, 34–40. in Russian.

Aprelkov, S. E., Ivanov, B. V., & Popruzhenko, S. V. (1999). Tectonics and Geodynamic Evolution of Southeastern

Kamchatka (Petropavlovsk Geodynamic Ground). *Pacific Geology, 18*(4), 16–28. in Russian.

Aprelkov, S. Y., & Svyatlovsky, A. Y. (1989). The origin of Avacha Bay in Kamchatka. *Pacific Geology, 4*, 108–111. in Russian.

Avdeiko, G. P., & Bergal-Kuvikas, O. V. (2015). The geodynamic conditions for the generation of adakites and Nb-rich basalts (NEAB) in Kamchatka. *Journal of Volcanology and Seismology, 9*(5), 295–306. https://doi.org/10.1134/S0742046315050024

Avdeiko, G. P., Palueva, A. A., & Khleborodova, O. A. (2006). Geodynamic conditions of volcanism and magma formation in the Kurile-Kamchatka island-arc system. *Petrology, 14*(3), 230–246. https://doi.org/10.1134/S0869591106030027

Balyev, EYu., Perepelov, A. B., Ananev, V. V., & Taktaev, B. N. (1984). High alkaly andesites in frontal part of island arc (Kamchatka). *Report of Academy USSR, 274*(4), 977–981. in Russian.

Barde-Cabusson, S., Gottsmann, J., Martí, et al. (2014). Structural control of monogenetic volcanism in the Garrotxa volcanic field (Northeastern Spain) from gravity and self-potential measurements. *Bulletin of Volcanology, 76*(1), 788. https://doi.org/10.1007/s00445-013-0788-0

Bazanova, L. I., Puzankov, M. Yu., Dirksen, O. V., Kulich, R. P., & Kartasheva, E. V. (2012). Lava flows of Koryaksky volcano in Holocene: success and problems of the dating. *Materials of the annual volcanologist day «Volcanism and related process».* Petropavlovsk-Kamchatsky (pp. 11–18) (**in Russian**).

Ben-Avraham, Z. V. I., Nur, A., Jones, D., & Cox, A. (1981). Continental accretion: From oceanic plateaus to allochthonous terranes. *Science, 213*(4503), 47–54. https://doi.org/10.1126/science.213.4503.47

Bergal-Kuvikas, O., Bindeman, I., Chugaev, A., Larionova, Yu., Khubaeva, O., & Perepelov, A. (2021). Monogenetic volcanism at Malko-Petropavlovsk zone of the transverse dislocation (Kamchatka). *Mendeley Data.* https://doi.org/10.17632/8d69jr8yjv.1

Bergal-Kuvikas, O., Leonov, V., Rogozin, A., Bindeman, I., Kliapitskiy, E., & Churikova, T. (2019). Stratigraphy, structure and geology of Late Miocene Verkhneavachinskaya caldera with basaltic–andesitic ignimbrites at Eastern Kamchatka. *Journal of Geosciences, 64*, 229–250. https://doi.org/10.3190/jgeosci.295

Bergal-Kuvikas, O., Nakagawa, M., Kuritani, T., et al. (2017). A petrological and geochemical study on time-series samples from Klyuchevskoy volcano, Kamchatka arc. *Contributions to Mineralogy and Petrology, 172*(5), 35. https://doi.org/10.1007/s00410-017-1347-z

Bindeman, I. N., Anikin, L. P., & Schmitt, A. K. (2016). Archean Xenocrysts in Modern Volcanic Rocks from Kamchatka: Insight into the Basement and Paleodrainage. *Journal of Geology, 124*(2), 247–253. https://doi.org/10.1086/684833

Bindeman, I. N., Vinogradov, V. I., Valley, J. W., Wooden, J. L., & Natalin, B. A. (2002). Archean protolith and accretion of crust in Kamchatka: SHRIMP dating of zircons from metamorphic rocks of Sredinny and Ganal Massifs. *Journal of Geology, 110*, 271–289. https://doi.org/10.1086/339532

Bushenkova, N., Koulakov, I., Senyukov, S., et al. (2019). Tomographic images of magma chambers beneath the Avacha and Koryaksky volcanoes in Kamchatka. *Journal of Geophysical Research: Solid Earth, 124*(9), 9694–9713. https://doi.org/10.1029/2019JB017952

Calmus, T., Pallares, C., Maury, R. C., et al. (2011). Volcanic markers of the post-subduction evolution of Baja California and Sonora, Mexico: Slab tearing versus lithospheric rupture of the Gulf of California. *Pure and Applied Geophysics, 168*(8), 1303–1330. https://doi.org/10.1007/s00024-010-0204-z

Chebrova, A. Y., Chemarev, A. S., Matveenko, E. A., & Chebrov, D. V. (2020). Seismological data information system in Kamchatka branch of GS RAS: Organization principles, main elements and key functions. *Geophysical Research, 21*(3), 66–91.

Chebrov, V. N., Droznin, D. V., Kugaenko, Y. A., et al. (2013). The system of detailed seismological observations in Kamchatka in 2011. *Journal of Volcanology and Seismology, 7*(1), 16–36. https://doi.org/10.1134/S0742046313010028

Chekhovich, V. D., & Sukhov, A. N. (2006). Breakup of the Late Cretaceous Achaivayam-Valagin volcanic arc in the Paleocene (terranes of southern Koryakia and eastern Kamchatka). *Doklady Earth Sciences, 409*(2), 893. https://doi.org/10.1134/S1028334X06060122

Chernyshev, I. V., Chugaev, A. V., & Shatagin, K. N. (2007). High-precision Pb isotope analysis by multicollector-ICP-mass-spectrometry using 205Tl/203Tl normalization: Optimization and calibration of the method for the studies of Pb isotope variations. *Geochemistry International, 45*, 1065–1076. https://doi.org/10.1134/S0016702907110018

Chudaev, O. V., Chelnokov, G. A., Bragin, I. V., et al. (2016). Geochemical features of major and rare-earth element behavior in the Paratunka and Bol'shebannyi hydrothermal systems of Kamchatka. *Russian Journal of Pacific Geology, 10*(6), 458–475. https://doi.org/10.1134/S1819714016060026

Chudaev, O.V., Chudaeva, V.A., Karpov, G.A., & Edmunds, S.P. (2000). Geochemistry of water of the basic geothermal area of Kamchatka. *Dalnauka.* Vladivostok. (p. 157) (**in Russian**).

Chugaev, A. V., Chernyshev, I. V., Lebedev, V. A., & Eremina, A. V. (2013). Lead Isotope composition and origin of the quaternary lavas of Elbrus Volcano, the Greater Caucasus: High-precision MC-ICP-MS data. *Petrology, 21*, 16–27. https://doi.org/10.1134/S0869591113010037

Churikov, V. A., & Kuzmin, Y. O. (1998). Relation between deformation and seismicity in the active fault zone of Kamchatka, Russia. *Geophysical Journal International, 133*(3), 607–614. https://doi.org/10.1046/j.1365-246X.1998.00511.x

Churikova, T., Dorendorf, F., & Wörner, G. (2001). Sources and fluids in the mantle wedge below Kamchatka, evidence from across-arc geochemical variation. *Journal of Petrology, 42*(8), 1567–1593. https://doi.org/10.1093/petrology/42.8.1567

Connor, C. B., Conway, F. M., & Sigurdsson, H. (2000). Basaltic volcanic fields. *Encyclopedia of Volcanoes*, 331–343.

Dirksen, O. V. (2009). Late Quaternary Areal Volcanism of Kamchatka. *Doctoral dissertation*, Sankt-Petersburg State University (p. 171) (**in Russian**).

Dmitriev, V. D., & Ezhov, B. V. (1977). About question of genesis of Avacha bay. *Questions of Geography of Kamchatka, 7*, 45–47. in Russian.

Dorendorf, F., Churikova, T., Koloskov, A., & Wörner, G. (2000). Late Pleistocene to Holocene activity at Bakening volcano and surrounding monogenetic centers (Kamchatka): Volcanic geology and geochemical evolution. *Journal of Volcanology and Geothermal Research, 104*(1–4), 131–151. https://doi.org/10.1016/S0377-0273(00)00203-1

Dubik, Yu. M., & Ogorodov, N. V. (1970). Volcanic cone in Avacha bay. *Questions of Geography of Kamchatka, 6*, 171–172. in Russian.

Duggen, S., Portnyagin, M., Baker, J., et al. (2007). Drastic shift in lava geochemistry in the volcanic-front to rear-arc region of the Southern Kamchatkan subduction zone: Evidence for the transition from slab surface dehydration to sediment melting. *Geochimica Et Cosmochimica Acta, 71*(2), 452–480. https://doi.org/10.1016/j.gca.2006.09.018

Emelyanova, T. A., & Lelikov, E. P. (2013). Volcanism as an indicator of a depth mechanism for the formation of the Seas of Japan and Okhotsk. *Russian Journal of Pacific Geology, 7*(2), 124–132. https://doi.org/10.1134/S1819714013020036

Favorskaya, M. A., Volchanskaya, I. K., Frich-har, D. I., Baskina, V. A., & Dudykina, A. S. (1965). Magmatism of south-east Kamchatka and their relation with tectonic activation. Moscow. Nauka. p. 151 (**in Russian**).

Federal State Statistics Service. https://eng.gks.ru. Accessed 26 Oct 2020.

Ferrari, L., Rosas-Elguera, J., Delgado-Granados, H. (2000). *Late Miocene to Quaternary extension at the northern boundary of the Jalisco block, western Mexico: The Tepic-Zacoalco rift revised*. Special papers. Geologicl society of America. (pp. 41–64).

Florensky, I. V., & Bazanova, L. I. (1989). Volcanism during cenozoic time in South-East of Kamchatka (Beregovoy ridge). *Volcanology and Seismology, 6*, 30–41. in Russian.

Gall, H., Furman, T., Hanan, B., et al. (2021). Post-delamination magmatism in south-central Anatolia. *Lithos*. https://doi.org/10.1016/j.lithos.2021.106299

Gazel, E., Carr, M. J., Hoernle, K., Feigenson, et al. (2009). Galapagos-OIB signature in southern Central America: Mantle refertilization by arc–hot spot interaction. *Geochemistry, Geophysics, Geosystems*. https://doi.org/10.1029/2008GC002246

Geological, geophysical atlas of the Kurile Kamchatka island arc. (1987). *VSEGEI*. Leningrad (pp. 36) (**in Russian**).

Geological map of Russian Federation. (2000). Scale 1:200 000. Issue Sothern Kamchatka. Lists N-57-XXVII, N-57-XXXIII. VSEGEI. Sankt-Petersburg (**in Russian**).

Geology of USSR. (1967). XXXI. Kamchatka, Komandor and Kurile islands. G.M. Vlasov (Ed.). Moscow. Nedra (p. 733) (**in Russian**)

Global volcanism program (GVP). (2021). https://volcano.si.edu. Accessed 01 Mar 2021.

Gontovaya, L. I., Popruzhenko, S. V., & Nizkous, I. V. (2010). Upper mantle structure in the ocean-continent transition zone: Kamchatka. *Journal of Volcanology and Seismology, 4*(4), 232–247. https://doi.org/10.1134/S0742046310040020

Gorbatov, A., Kostoglodov, V., Suárez, G., & Gordeev, E. (1997). Seismicity and structure of the Kamchatka subduction zone. *Journal of Geophysical Research: Solid Earth, 102*(B8), 17883–17898. https://doi.org/10.1029/96JB03491

Gordeev, E. I., & Bergal-Kuvikas, O. V. (2022). Structure of subduction zone and volcanism on Kamchatka. *Doklady of the Earth Sciences, 2*(502), 26–30. https://doi.org/10.31857/S2686739722020086

Grib, E. N. (1985). The andesites of Mount Mishennaya. *Questions of Geography of Kamchatka, 9*, 130–133. in Russian.

Grib, E. N., Delemen, I. F., & Fedotov, S. A. (1986). The Structure, Composition, and Origin of the Andesite Dome of Mount Mishennaya, Kamchatka. *Vulkanologiya i Seismologiya, 6*, 29–44 (**in Russian**).

Gutiérrez, F., Gioncada, A., Ferran, O. G., Lahsen, A., & Mazzuoli, R. (2005). The Hudson Volcano and surrounding monogenetic centres (Chilean Patagonia): An example of volcanism associated with ridge–trench collision environment. *Journal of Volcanology and Geothermal Research, 145*(3–4), 207–233. https://doi.org/10.1016/j.jvolgeores.2005.01.014

Hamilton, W. B. (1994). Subduction systems and magmatism. *Geological Society, London, Special Publications, 81*(1), 3–28.

Hart, S. R. (1984). A large-scale isotope anomaly in the Southern Hemisphere mantle. *Nature, 309*(5971), 753–757. https://doi.org/10.1038/309753a0

Helz, R. T., & Thornber, C. R. (1987). Geothermometry of Kilauea Iki lava lake, Hawaii. *Bulletin of volcanology*, *49*(5), 651–668.

Holocene volcanism of Kamchatka. http://geoportal.kscnet.ru/volcanoes/geoservices/hvolc. Accessed 21 Oct 2020.

Hourigan, J. K., Brandon, M. T., Soloviev, A. V., et al. (2009). Eocene arc-continent collision and crustal consolidation in Kamchatka, Russian Far East. *American Journal of Science, 309*, 333–396. https://doi.org/10.2475/05.2009.01

Johnston, S. T., & Thorkelson, D. J. (1997). Cocos-Nazca slab window beneath central America. *Earth and Planetary Science Letters, 146*(3–4), 465–474. https://doi.org/10.1016/S0012-821X(96)00242-7

Khanchuk, A. I., Kemkin, I. V., & Kruk, N. N. (2016). The Sikhote-Alin orogenic belt, Russian South East: Terranes and the formation of continental lithosphere based on geological and isotopic data. *Journal of Asian Earth Sciences, 120*, 117–138. https://doi.org/10.1016/j.jseaes.2015.10.023

Kimura, J. I., & Yoshida, T. (2006). Contributions of slab fluid, mantle wedge and crust to the origin of Quaternary lavas in the NE Japan arc. *Journal of Petrology, 47*(11), 2185–2232. https://doi.org/10.1093/petrology/egl041

Kinoshita, O. (1999). A migration model of magmatism explaining a ridge subduction, and its details on a statistical analysis of the granite ages in Cretaceous Southwest Japan. *The Island Arc, 8*, 181–189. https://doi.org/10.1046/j.1440-1738.1999.00230.x

Konstantinovskaya, E. (2011). Early Eocene arc–continent collision in Kamchatka, Russia: structural evolution and geodynamic model. *Arc-Continent Collision*. https://doi.org/10.1007/978-3-540-88558-0_9

Koyama, M., & Umino, S. (1991). Why does the Higashi-Izu monogenetic volcano group exist in the Izu Peninsula? Relationships between late Quaternary volcanism and tectonics in the northern tip of the Izu-Bonin arc. *Journal of Physics of the Earth, 39*(1), 391–420. https://doi.org/10.4294/jpe1952.39.391

Kozhurin, A. I., Ponomareva, V. V., & Pinegina, T. K. (2008). Active faulting in the south of Central Kamchatka. *Bulletin of Kamchatka Regional Association Educational-Scientific Center. Earth Sciences, 2*, 10–27. in Russian.

Kozhurin, A., & Zelenin, E. (2017). An extending island arc: The case of Kamchatka. *Tectonophysics, 706*, 91–102. https://doi.org/10.1016/j.tecto.2017.04.001

Krasheninnikov, S. P., Bazanova, L. I., Ponomareva, V. V., & Portnyagin, M. V. (2020). Detailed tephrochronology and composition of major Holocene eruptions from Avachinsky, Kozelsky, and Koryaksky volcanoes in Kamchatka. *Journal of Volcanology and Geothermal Research*. https://doi.org/10.1016/j.jvolgeores.2020.107088

Krohin, E. M. (1954). About sone volcanic structures in valley of Malaya Bustraya, Levaya Topolovaya, Bolshaya Saranaya. *Bulleten of Volcanological Station, 22*, 39–43. in Russian.

Lander, A. V., & Shapiro, M. N. (2007). The origin of the modern Kamchatka subduction zone. *Washington DC American Geophysical Union Geophysical Monograph Series, 172*, 57–64. https://doi.org/10.1029/172GM05

Larionova, Y. O., Samsonov, A. V., & Shatagin, K. N. (2007). Sources of Archean sanukitoids (high-Mg subalkaline granitoids) in the Karelian Craton: Sm-Nd and Rb-Sr isotopic-geochemical evidence. *Petrology, 15*(6), 530–550. https://doi.org/10.1134/S0869591107060021

Le Corvec, N., Spörli, K. B., Rowland, J., & Lindsay, J. (2013). Spatial distribution and alignments of volcanic centers: Clues to the formation of monogenetic volcanic fields. *Earth-Science Reviews, 124*, 96–114. https://doi.org/10.1016/j.earscirev.2013.05.005

Leonov, V. L., & Rogozin, A. N. (2007). Karymshina, a giant supervolcano caldera in Kamchatka: Boundaries, structure, volume of pyroclastics. *Journal of Volcanology and Seismology, 1*(5), 296–309. https://doi.org/10.1134/S0742046307050028

Levashova, N. M., Shapiro, M. N., Beniamovsky, V. N., & Bazhenov, M. L. (2000). Paleomagnetism and geochronology of the Late Cretaceous-Paleogene island arc complex of the Kronotsky Peninsula, Kamchatka, Russia: Kinematic implications. *Tectonics, 19*(5), 834–851. https://doi.org/10.1029/1998TC001087

Loginov, V.A., Gontovaya, L.I. (2020). Structure of the lithosphere in Avacha-Koryak group of volcano based on geohysical data (Kamchatka). *Annual conference to volcanological day «Volcanism and related process»* (pp. 107–109) (**in Russian**).

Lustrino, M., Keskin, M., Mattioli, M., et al. (2010). Early activity of the largest Cenozoic shield volcano in the circum-Mediterranean area: Mt. Karacadag, SE Turkey. *European Journal of Mineralogy, 22*(3), 343–362. https://doi.org/10.1127/0935-1221/2010/0022-2024

Maccaferri, F., Acocella, V., & Rivalta, E. (2015). How the differential load induced by normal fault scarps controls the distribution of monogenic volcanism. *Geophysical Research Letters, 42*(18), 7507–7512. https://doi.org/10.1002/2015GL065638

Marrett, R., & Allmendinger, R. W. (1992). Amount of extension on "small" faults: An example from the Viking graben. *Geology, 20*(1), 47–50. https://doi.org/10.1130/0091-7613(1992)020%3c0047:AOEOSF%3e2.3.CO;2

Martí, J., López, C., Bartolini, S., Becerril, L., & Geyer, A. (2016). Stress controls of monogenetic volcanism: A review. *Frontiers in Earth Science, 4*, 106. https://doi.org/10.3389/feart.2016.00106

Masurenkov, Y. P., Egorova, I. A., & Puzankov, M. Y. (1991). Avachinsky Volcano: Kamchatka active volcanoes. *Active Volcanoes of Kamchatka, 2*, 246–273. in Russian.

McCrory, P. A., Wilson, D. S., & Stanley, R. G. (2009). Continuing evolution of the Pacific-Juan de Fuca-North America slab window system—A trench–ridge–transform example from the Pacific Rim. *Tectonophysics, 464*(1–4), 30–42. https://doi.org/10.1016/j.tecto.2008.01.018

Mitichkin, M. A., Perepelov, A. B., Dril, S. I., Chuvashova, L. A., & Smirnova, E. V. (1998). Rare Earth Elements and the Geochemical Typification of Intrusive Rocks from the Malka-Petropavlovsk Transverse Fault Zone, Kamchatka. *Doklady Earth Sciences, 362*(7), 974–977. in Russian.

Miyashiro, A. (1974). Volcanic rock series in island arcs and active continental margins. *American Journal of Science, 274*(4), 321–355. https://doi.org/10.2475/ajs.274.4.321

Moroz, Y. F., & Gontovaya, L. I. (2003). Deep structure of Avachinsky-Koryaksky group of volcanoes. *Volcanology and Seismology, 4*, 3–10. in Russian.

Moroz, Y. F., & Gontovaya, L. I. (2018). Deep structure of South Kamchatka according to geophysical data. *Geodynamics & Tectonophysics, 9*(4), 1147–1161. https://doi.org/10.5800/GT-2018-9-4-0387

Nakamura, K. (1977). Volcanoes as possible indicators of tectonic stress orientation principle and proposal. *Journal of Volcanology and Geothermal Research, 2*, 1–16. https://doi.org/10.1016/0377-0273(77)90012-9

Németh, K. (2010). Monogenetic volcanic fields: Origin, sedimentary record, and relationship with polygenetic volcanism. *What is a Volcano?* (vol. 470, p. 43).

Németh, K., & Kereszturi, G. (2015). Monogenetic volcanism: Personal views and discussion. *International Journal of Earth Sciences, 104*(8), 2131–2146. https://doi.org/10.1007/s00531-015-1243-6

Nieto-Samaniego, Á. F., Ferrari, L., Alaniz-Alvarez, S. A., Labarthe-Hernández, G., & Rosas-Elguera, J. (1999). Variation of Cenozoic extension and volcanism across the southern Sierra Madre Occidental volcanic province, Mexico. *Geological Society of America Bulletin, 111*(3), 347–363. https://doi.org/10.1130/0016-7606(1999)111%3c0347:VOCEAV%3e2.3.CO;2

Nurmukhamedov, A. G., & Sidorov, M. D. (2019). Deep structure and geothermal potential along the regional profile set from Opala Mountain to Vakhil'River (Southern Kamchatka). *IOP Conference Series: Earth and Environmental Science, 249*(1), 012041. https://doi.org/10.1088/1755-1315/249/1/012041

Oyan, V., Keskin, M., Lebedev, V. A., et al. (2017). Petrology and Geochemistry of the Quaternary Mafic Volcanism to the NE of Lake Van, Eastern Anatolian Collision Zone, Turkey. *Journal of Petrology, 58*(9), 1701–1728. https://doi.org/10.1093/petrology/egx070

Pardo, N., Macias, J. L., Giordano, G., Cianfarra, P., Avellán, D. R., & Bellatreccia, F. (2009). The $\sim$ 1245 yr BP Asososca maar eruption: The youngest event along the Nejapa-Miraflores volcanic fault, Western Managua, Nicaragua. *Journal of Volcanology and Geothermal Research, 184*(3–4), 292–312. https://doi.org/10.1016/j.jvolgeores.2009.04.006

Pearce, J. A. (2008). Geochemical fingerprinting of oceanic basalts with applications to ophiolite classification and the search for Archean oceanic crust. *Lithos, 100*(1–4), 14–48. https://doi.org/10.1016/j.lithos.2007.06.016

Pinegina, T. K., Bazanova, L. I., Zelenin, E. A., et al. (2018). Holocene Tsunamis in Avachinsky Bay, Kamchatka, Russia. *Pure and Applied Geophysics, 175*(4), 1485–1506. https://doi.org/10.1007/s00024-018-1830-0

Ponomareva, V. V., Melekestsev, I. V., & Dirksen, O. V. (2006). Sector collapses and large landslides on Late Pleistocene-Holocene volcanoes in Kamchatka, Russia. *Journal of Volcanology and Geothermal Research, 158*(1–2), 117–138. https://doi.org/10.1016/j.jvolgeores.2006.04.016

Popruzhenko, S. V., & Zubin, M. I. (1997). Tectonics and some features of seismicity of the shelf zone of the Avacha Bay and adjacent areas. *Volcanology and Seismology., 2*, 74–81. in Russian.

Putirka, K. D. (2008). Thermometers and barometers for volcanic systems. *Reviews in Mineralogy and Geochemistry, 69*(1), 61–120. https://doi.org/10.2138/rmg.2008.69.3

Rehkämper, M., & Halliday, A. M. (1998). Accuracy and long-term reproducibility of lead isotopic measurements by MC-ICP-MS using an external method for correction of mass discrimination. *International Journal of Mass Spectrometry, 181*, 123–133. https://doi.org/10.1016/S1387-3806(98)14170-2

Seismological data information system KBGS RAS. http://sdis.emsd.ru/info/earthquakes/catalogue.php. Accessed 1 Nov 2020.

Seliverstov, N.I. (1998). *The Kamchatka Offshore and Geodynamics of the Kuriles-Kamchatka and the Aleutian Junction*. Nauchnyi Mir, Moscow (**in Russian**).

Seliverstov, N. I. (2009). *Geodynamics of the Junction Zone of the Kuril–Kamchatka and Aleutian Island Arc*. Petropavlovsk-Kamchatsky: KamGU (p. 191) (**in Russian**).

Shatser, A.E. (1987). Cainozoic development of Kamchatka—formation and destruction unstable orogenic uplifts. In *Essays of tectonic development of Kamchatka (Belousov V.V. edt)*. Nauka. M. (pp. 109–164) (**in Russian**).

Sheimovich, V. S., Golovin, D. I., & Gertsev, D. O. (2007). The andesite extrusion of Mount Mishennaya, Kamchatka, and its age. *Journal of Volcanology and Seismology, 1*(4), 248–253. https://doi.org/10.1134/S0742046307040033

Sheimovich, V.S., & Patoka, M.G. (2000). Geological setting of zones with active cenozoic volcanism. Moscow: Geos, 208 (**in Russian**).

Sheimovich, V. A., Puzankov, Yu. M., Puzankov, MYu., Golovin, D. I., Bobrov, V. A., & Moskaleva, S. V. (2005). Manifestations of alkaline magmatism in the Avacha bay area. *Volcanology and Seismilogy, 36*(6), 36–46. in Russian.

Sheimovich, V. S., & Sidorov, M. D. (2000). Structure of the basement under the southest Kamchatka volcanic belt. *Volcanology and Seismology, 5*, 28–35. in Russian.

Smith, I. E., Brenna, M., & Cronin, S. J. (2021). The magma source of small-scale intraplate monogenetic volcanic systems in northern New Zealand. *Journal of Volcanology and Geothermal Research, 418*, 107326. https://doi.org/10.1016/j.jvolgeores.2021.107326

Smith, I. E. M., & Németh, K. (2017). Source to surface model of monogenetic volcanism: A critical review. *Geological Society, London, Special Publications, 446*(1), 1–28. https://doi.org/10.1144/SP446.14

Sugrobov, V. M., & Yanovsky, F. A. (1991). Geothermal field of Kamchatka., heat Losses by volcanoes and hydroterms. In *Active volcanoes of Kamchatka*. S.A. Fedotov, & Yu.P. Masurenkov (Eds.) (vol. 1, pp. 67–74).

Sun, S. S., & McDonough, W. F. (1989). Chemical and isotopic systematics of oceanic basalts: Implications for mantle composition and processes. *Geological Society, London, Special Publications, 42*(1), 313–345. https://doi.org/10.1144/GSL.SP.1989.042.01.19

Svyatlovsky, A. E. (1956). Yuzhno-Bustrinsky range. *Works of Volcanology Laboratory, 12*, 110–190. in Russina.

Syracuse, E. M., & Abers, G. A. (2006). Global compilation of variations in slab depth beneath arc volcanoes and implications. *Geochemistry, Geophysics, Geosystems*. https://doi.org/10.1029/2005GC001045

Takada, A. (1994). The influence of regional stress and magmatic input on styles of monogenetic and polygenetic volcanism. *Journal of Geophysical Research: Solid Earth, 99*(B7), 13563–13573.

Tsukanov, N. V., Palechek, T. N., Soloviev, A. V., & Savelyev, D. P. (2014). Tectono-stratigraphic complexes of the southern segment of the Kronotsky paleoarc (East Kamchatka): Their structure, age, and composition. *Pacific Geology, 6*(33), 3–17. in Russian.

Valentine, G. A., & Connor, C. B. (2015). Basaltic volcanic fields. In *The encyclopedia of volcanoes* (pp. 423–439). Academic Press.

Yamasaki, T., & Gernigon, L. (2009). Styles of lithospheric extension controlled by underplated mafic bodies. *Tectonophysics, 468*(1–4), 169–184. https://doi.org/10.1016/j.tecto.2008.04.024